A WIND-TUNNEL INVESTIGATION OF AN UNPOWERED HELICOPTER FUSELAGE MODEL WITH A V-TYPE EMPENNAGE

Carl E. Freeman and William T. Yeager, Jr.

Langley Directorate,
U.S. Army Air Mobility R&D Laboratory
Langley Research Center
Hampton, Va. 23665

NATIONAL AERONAUTICS AND SPACE ADMINISTRATION • WASHINGTON, D. C. • MARCH 1977

1. Report No.	2. Government Accession No.	3. Recipient's Catalog No.
NASA TM X-3476		

4. Title and Subtitle	5. Report Date
WIND-TUNNEL INVESTIGATION OF AN UNPOWERED HELICOPTER FUSELAGE MODEL WITH V-TYPE EMPENNAGE	March 1977
	6. Performing Organization Code
7. Author(s)	8. Performing Organization Report No.
Carl E. Freeman and William T. Yeager, Jr.	L-11273
	10. Work Unit No. 505-10-21-03
9. Performing Organization Name and Address	11. Contract or Grant No.
Langley Directorate, USAAMRDL NASA Langley Research Center Hampton, VA 23665	
	13. Type of Report and Period Covered
12. Sponsoring Agency Name and Address	Technical Memorandum
National Aeronautics and Space Administration Washington, DC 20546 and U.S. Army Air Mobility R&D Laboratory Moffett Field, CA 94035	14. Army Project No. 1L262209AH76

15. Supplementary Notes

Carl E. Freeman and William T. Yeager, Jr.: Langley Directorate, U.S. Army Air Mobility R&D Laboratory.

16. Abstract

An investigation has been undertaken to establish the applicability of a V-type empennage on an unpowered semiscale helicopter fuselage. Configuration changes included variations of V-tail dihedral angle, planform area, and incidence angle. Of the configurations tested, a V-tail with a dihedral angle of 55°, a total planform area of 0.244 m^2 (2.625 ft^2), and an incidence angle of 5° most nearly match the trim and static stability of the baseline conventional empennage.

This paper is applicable to design criteria for improved directional control devices.

17. Key Words (Suggested by Author(s))	18. Distribution Statement
Helicopter V-tail Empennage Static stability	Unclassified - Unlimited Subject Category 02

19. Security Classif. (of this report)	20. Security Classif. (of this page)	21. No. of Pages	22. Price*
Unclassified	Unclassified	52	$4.25

*For sale by the National Technical Information Service, Springfield, Virginia 22161

WIND-TUNNEL INVESTIGATION OF AN UNPOWERED HELICOPTER FUSELAGE MODEL WITH V-TYPE EMPENNAGE

Carl E. Freeman* and William T. Yeager, Jr.*
Langley Research Center

SUMMARY

An investigation has been undertaken to establish the applicability of a V-type empennage on an unpowered semiscale helicopter fuselage. Configuration changes included variations of V-tail dihedral angle, planform area, and incidence angle. Of the configurations tested, a V-tail with a dihedral angle of 55°, a total planform area of 0.244 m^2 (2.625 ft^2), and an incidence angle of 5° most nearly match the trim and static stability of the baseline conventional empennage.

INTRODUCTION

Conventionally powered, single rotor helicopters have experienced directional control problems while operating in low-velocity left rear quartering winds in ground effect and during low-speed sideward flight in ground effect (refs. 1 and 2). Investigations have been conducted to determine the source of these directional control problems and possible means of alleviating them (refs. 3 to 5). Reference 4 showed that a V-type empennage presents significant advantages over conventional horizontal-vertical control surfaces with respect to helicopter directional control at low speeds. The principal advantages are: (1) smaller adverse fin forces and (2) increased tail-rotor efficiency.

To investigate more fully the effects of a V-type empennage on vehicle stability and control at typical helicopter cruise speeds, a parametric study was conducted in the Langley V/STOL tunnel. The tests were carried out with an unpowered helicopter fuselage model to provide a baseline for V-type and conventional empennage static stability comparisons. V-tail parameters investigated were planform area, dihedral angle, and incidence angle.

SYMBOLS

Units used for the physical quantities defined in this paper are given in the International System of Units (SI) and parenthetically in U.S. Customary Units. Measurements and calculations were made in U.S. Customary Units. Conversion factors are presented in reference 6.

Positive senses of forces, moments, and angles are presented in figure 1. Relative balance positions and location of the model moment reference center are shown in figure 2.

---

*Langley Directorate, U.S. Army Air Mobility R&D Laboratory.

A	reference rotor disk area, πR^2
C_D	drag coefficient, $\frac{F_D}{q_\infty A}$
C_L	lift coefficient, $\frac{F_L}{q_\infty A}$
C_l	rolling-moment coefficient, $\frac{M_X}{q_\infty AR}$
C_m	pitching-moment coefficient, $\frac{M_Y}{q_\infty AR}$
C_n	yawing-moment coefficient, $\frac{M_Z}{q_\infty AR}$
C_Y	side-force coefficient, $\frac{F_Y}{q_\infty A}$
c_l	section lift coefficient
F_D	drag force, N (lbf)
F_L	lift force, N (lbf)
F_Y	side force, N (lbf)
i_H	horizontal-tail incidence angle, deg
i_V	V-tail incidence angle, deg
M_X	rolling moment, N-m (ft-lb)
M_Y	pitching moment, N-m (ft-lb)
M_Z	yawing moment, N-m (ft-lb)
q_∞	dynamic pressure, Pa (psf)
R	reference rotor radius, 1.68 m (5.5 ft)
S	V-tail total planform area, m^2 (ft^2)
V_∞	free-stream velocity, m/sec (ft/sec)
α	angle of attack, deg
β	angle of sideslip, deg
Γ	dihedral angle, deg

ϕ roll angle, deg

Model component designations:

F fuselage

G landing skids

S conventional empennage

W wing

V_{abc} V-tail empennage, where a, b, and c are as indicated in the following table:

a	Γ, deg	b	S, m^2 (ft^2)	c	i_V, deg
1	45	1	0.186 (2.000)	1	5
2	50	2	.244 (2.625)	2	8
3	55	3	.302 (3.250)	3	10

Abbreviation:

W.L. water line

MODEL AND APPARATUS

A photograph of the model used in this investigation is shown in figure 3. Dimensions and geometric characteristics are given in table I. The total model system consisted of a fuselage-empennage combination configured to represent the attack helicopter of reference 1, the general rotor model system (GRMS), and the Langley V/STOL tunnel high alpha-beta sting assembly.

Figure 2 illustrates the differences between the model used in this investigation and an exact 1/4-scale model of the attack helicopter of reference 1. The model fuselage width was increased to accommodate the GRMS. All other components: pylon, landing skids, wings, and empennage were true 1/4 scale.

The GRMS consists of a strain-gage balance system and a rotor power system. Three six-component strain-gage balances were used to measure aerodynamic forces and moments on the model. The main balance measured total model forces and moments. The rotor balance was mounted inside the model and measured loads on the rotor hub and shaft. The tail balance was mounted on the aft part of the GRMS keel and measured the empennage aerodynamic loads, including 33.0 cm (13.0 in.) of the tail cone.

The model was supported at a 10° angle from the bottom by the high alpha-beta sting assembly (fig. 3). The desired pitch and sideslip angles were obtained by varying the three sting joint angles. Model height above the tunnel floor remained constant, and model roll angle remained nominally 0°. The model pitch and roll angles were measured by instrumentation inside the model, and

model sideslip angle was calculated from the relationship of the three sting joint angles.

The model could be configured with either a conventional or V-tail empennage. The conventional empennage consisted of a horizontal and vertical stabilizer. The horizontal surfaces had negative camber with a variable incidence capability. The vertical tail had negative camber (positive side force) and fixed incidence. The V-tail empennage could be configured with three surface areas, three dihedral angles, and three incidence angles. Details of this empennage are shown in figure 4. Strain gages were attached to the spars of the V-tail panels to measure beamwise loads on the individual panels. The right V-panel, as well as the conventional vertical tail, had representative tail-rotor gearbox fairings.

During part of the investigation, the V-tail empennage was mounted alone with the tail balance on a blade strut to obtain tail data without fuselage interference. A bluff forebody was attached to the strut to close off the tail cone. A photograph of this arrangement is presented in figure 5.

TESTS AND CORRECTIONS

The tests were conducted in the Langley V/STOL tunnel, which is an atmospheric, closed-circuit wind tunnel. The test section measures 4.42 m (14.50 ft) by 6.63 m (21.75 ft). During the tests, the model was held near the center line of the test section out of ground effect. Data were obtained at free-stream dynamic pressures of 694, 1436, 1896, and 2298 Pa (14.5, 30.0, 39.6, and 48.0 psf) which correspond to a Mach number range of 0.10 to 0.18. Transition grit was placed on the fuselage, wings, and tail surfaces, as suggested in reference 7.

Angle-of-attack sweeps were made at 0° sideslip from -18° to 8° beginning at 0° angle of attack. Sideslip sweeps were made at nominal fuselage trim pitch angles for each particular airspeed. These trim conditions were based on 1g level flight with a two-bladed teetering rotor and were determined using the computer program described in references 8 to 10.

All data have been corrected for jet-boundary effects by the methods used in reference 11. Longitudinal and directional corrections were applied to the main and tail balance data to account for the movement of the middle section of the model support sting. Depending upon the pitch and yaw angles required and the tunnel dynamic pressure, the sting caused a variable flow deflection at the tail. By holding the pitch and yaw angles constant and by moving the middle section of the sting around its azimuth, the flow-field variations were obtained and corrections were applied to the data.

The data were recorded on a digital data-acquisition system. A data point consisted of an average of fifty samples of data acquired over a 5-sec interval. All strain-gage data were filtered above 2 Hz.

PRESENTATION OF DATA

Data taken during this investigation have been plotted and are given in figures 6 to 14. Longitudinal and lateral data for all three balances are referenced to the moment-reference center shown in figure 2. Longitudinal data are in the stability-axis system, and lateral data are in the body-axis system. Both the longitudinal and lateral data use a nominal rotor disk area and rotor radius as reference area and length.

The data are presented in the following order:

DISCUSSION OF RESULTS

The data in this report are, on the whole, presented without detailed analyses or correlation with theory. The main impetus for this investigation was to determine the effects of a V-type empennage on the static stability characteristics of an unpowered helicopter fuselage and to identify a V-tail configuration that provides essentially the same level of static longitudinal and lateral-directional stability as the baseline configuration. The baseline configuration used was that of the attack helicopter of reference 1. Not all the possible combinations of V-tail dihedral angle, planform area, and incidence angle were tested. The configurations omitted were those that, based on data trends during the test, would not match the stability levels of the baseline configuration. The following sections are provided to describe highlights of the data presented.

Longitudinal Characteristics

Figures 6 to 8 show the effects of V-tail dihedral angle, planform area, and incidence angle on vehicle static longitudinal stability. Figure 6 shows that as the V-tail dihedral angle is increased for a fixed area, vehicle longitudinal stability decreases. This change is to be expected since an increase in dihedral angle results in a decrease in projected horizontal-tail area. This effect of dihedral angle is not as readily apparent in figures 6(a) and 6(b) as it is in figures 6(c) to 6(e) since the tail area of 0.186 m^2 (2.0 ft^2) appears to be marginal for producing positive longitudinal stability.

Figure 7 also shows the effect of V-tail planform area, for fixed dihedral angles, on vehicle longitudinal stability. As expected, increasing the area also increases the longitudinal stability. As figure 6 shows, the smallest V-tail area of the tests is marginal for producing positive longitudinal stability, particularly at positive angles of attack.

Figure 8 shows the effect of V-tail incidence angle on vehicle longitudinal stability for fixed values of dihedral angle and planform area. Changes in the incidence angle are shown to have little effect on the vehicle static longitudinal stability.

In figures 6 to 8 the longitudinal characteristics of the baseline vehicle configuration are compared with those of the V-tail configurations. The V-tail is shown to have stability characteristics generally as good as, or better than, the conventional tail arrangement used on the baseline vehicle configuration. This result is, of course, dependent on the combination of V-tail dihedral angle and planform area chosen. The smallest area tested is marginal even for the lowest dihedral angle, whereas the largest area tested produces more stability than needed even at the highest dihedral angle tested. The dihedral angle required to produce static longitudinal stability and trim essentially the same as the baseline configuration is dependent on the area chosen. The combination that produced longitudinal stability characteristics generally equivalent to the baseline configuration was a dihedral angle of 55°, a total planform area of 0.244 m^2 (2.625 ft^2), and an incidence angle of 5°.

The effect of the fuselage on vehicle longitudinal stability can also be determined from figures 6 to 8 by comparing the results from the total force and moment balance with the results from the tail balance. In all cases, the fuselage is seen to have a significant effect on vehicle longitudinal stability. This effect is particularly true for the baseline tail configuration. The V-tail is most affected by the fuselage when the smallest planform area is used.

As a means of verifying the adverse effect of the fuselage, several runs were made with the V-tail mounted alone in the test section as shown in figure 5. Results of these tests are presented in figure 9. These data show that the tail contribution to stability was considerably reduced because of the downwash effects associated with the fuselage-wing combination.

Figures 6 to 8 also show the drag characteristics of the baseline and V-tail configurations. The data show that the V-tail configuration generally produces more drag than the baseline configuration. This result may be caused by the increased area of the V-tail and by the interference and induced losses associated with the V-tail as indicated in reference 12.

Figure 10 summarizes data for the tail-off configuration and for the baseline configuration at several values of horizontal-tail incidence angle.

Lateral-Directional Characteristics

Figures 11 to 13 show the effects of V-tail dihedral angle, planform area, and incidence angle on vehicle static lateral and directional stability. Fig-

ure 11 shows that increasing V-tail dihedral angle, for a fixed planform area, has a small effect on the vehicle lateral and directional static stability. Figure 11 indicates that V-tail area is a more powerful parameter than dihedral angle.

Figure 12 shows the effect of V-tail area, for fixed dihedral angles, on vehicle lateral and directional static stability. Increasing the planform area while maintaining the dihedral angle increases both the lateral and directional stability. The smallest area is shown to be unsatisfactory regardless of the dihedral angle at which it is tested.

Figure 13 shows the effect of V-tail incidence angle, for fixed values of dihedral angle and planform area, on vehicle lateral and directional static stability. Changes in the incidence angle are shown to have little effect on the vehicle stability.

Figures 11 to 13 also show a comparison of the lateral and directional characteristics of the baseline configuration with each different V-tail configuration. With the exception of the smallest V-tail area of the tests, the V-tail is shown to have stability characteristics generally as good as, or better than, the conventional tail arrangement used on the baseline vehicle configuration. The small V-tail area produces sufficient lateral stability but does not always produce a stabilizing directional contribution. Just as for the vehicle longitudinal characteristics, the V-tail combination that produced lateral and directional stability characteristics generally equivalent to the baseline configuration was a dihedral angle of 55°, a total planform area of 0.244 m^2 (2.625 ft^2), and an incidence angle of 5°.

The fuselage effect on vehicle lateral and directional static stability can also be determined from figures 11 to 13 by comparing the results from the total force and moment balance with the results from the tail balance. Generally, the fuselage is found to have little or no effect on vehicle lateral stability but does produce a significant destabilizing effect directionally.

Figure 14 shows the effect of angle of attack on vehicle lateral and directional static stability characteristics. The vehicle is shown to have more favorable stability characteristics generally at negative angles of attack with the V-tail.

SUMMARY OF RESULTS

The results of this investigation of an unpowered helicopter model with a V-type empennage may be summarized as follows:

1. The V-tail dihedral angle needed to produce desired static stability characteristics is dependent on V-tail area.

2. For the dihedral angles tested, static lateral-directional stability was less sensitive than longitudinal stability to changes in dihedral angle.

3. For the range of V-tail parameters tested, the V-tail configuration produces higher drag than the baseline configuration.

4. A V-tail configuration with a dihedral angle of 55°, a total planform area of 0.244 m^2 (2.625 ft^2), and an incidence angle of 5° most nearly matched the trim and static stability of the baseline conventional empennage.

Langley Research Center
National Aeronautics and Space Administration
Hampton, VA 23665
February 4, 1977

REFERENCES

1. Connor, William J.: The Huey Cobra in Vietnam. 1968 Report to the Aerospace Profession, Tech. Rev., vol. 9, no. 2, Soc. Exp. Test Pilots, 1968, pp. 25-32.

2. Lynn, R. R.; Robinson, F. D.; Batra, N. N.; and Duhon, J. M.: Tail Rotor Design. Pt. I: Aerodynamics. J. Amer. Helicopter Soc., vol. 15, no. 4, Oct. 1970, pp. 2-15.

3. Huston, Robert J.; and Morris, Charles E. K., Jr.: A Wind-Tunnel Investigation of Helicopter Directional Control in Rearward Flight in Ground Effect. NASA TN D-6118, 1971.

4. Yeager, William T., Jr.; Young, Warren H., Jr.; and Mantay, Wayne R.: A Wind-Tunnel Investigation of Parameters Affecting Helicopter Directional Control at Low Speeds in Ground Effect. NASA TN D-7694, 1974.

5. Wiesner, Wayne; and Kohler, Gary: Tail Rotor Design Guide. USAAMRDL Tech. Rep. 73-99, U.S. Army, Jan. 1974. (Available from DDC as AD 775 391.)

6. Mechtly, E. A.: The International System of Units - Physical Constants and Conversion Factors (Second Revision). NASA SP-7012, 1973.

7. Braslow, Albert L.; and Knox, Eugene C.: Simplified Method for Determination of Critical Height of Distributed Roughness Particles for Boundary-Layer Transition at Mach Numbers From 0 to 5. NACA TN 4363, 1958.

8. Davis, John M.; Bennett, Richard L.; and Blankenship, Barney L.: Rotorcraft Flight Simulation With Aeroelastic Rotor and Improved Aerodynamic Representation. Volume I - Engineer's Manual. USAAMRDL-TR-74-10A, U.S. Army, June 1974. (Available from DDC as AD 782 854.)

9. Davis, John M.: Rotorcraft Flight Simulation With Aeroelastic Rotor and Improved Aerodynamic Representation. Volume II - User's Manual. USASMRDL-TR-74-10B, U.S. Army, June 1974. (Available from DDC as AD 782 756.)

10. Hsieh, P. Y.; and Davis, John M.: Rotorcraft Flight Simulation With Aeroelastic Rotor and Improved Aerodynamic Representations. Volume III - Programmer's Manual. USAAMRDL-TR-74-10C, U.S. Army, June 1974. (Available from DDC as AD 782 841.)

11. Gillis, Clarence L.; Polhamus, Edward C.; and Gray, Joseph L., Jr.: Charts for Determining Jet-Boundary Corrections for Complete Models in 7- by 10-Foot Closed Rectangular Wind Tunnels. NACA WR L-123, 1945. (Formerly NACA ARR L5G31.)

12. Hoerner, Sighard F.: Fluid-Dynamic Drag. Publ. by the author (148 Busteed Drive, Midland Park, New Jersey 07432), 1965.

TABLE I.- MODEL GEOMETRY

Wing:	
Airfoil:	
Root	NACA 0030
Tip	NACA 0024
Span, m (ft)	0.786 (2.58)
Area, m^2 (ft^2)	0.159 (1.71)
Chord:	
Root, m (ft)	0.213 (0.700)
Tip, m (ft)	0.158 (0.520)
Incidence angle (chord line), deg	14
Leading-edge sweep, deg	14
Dihedral angle, deg	0
Horizontal tail:	
Airfoil	Inverted Clark Y
Span, m (ft)	0.573 (1.88)
Area, m^2 (ft^2)	0.0975 (1.05)
Chord:	
Root, m (ft)	0.183 (0.60)
Tip, m (ft)	0.137 (0.45)
Incidence angle (chord line), deg	0, 6, 10
Leading-edge sweep, deg	20
Dihedral angle, deg	0
Vertical tail:	
Span, m (ft)	0.378 (1.24)
Area, m^2 (ft^2)	0.0966 (1.04)
Chord:	
Root, m (ft)	0.341 (1.12)
Tip, m (ft)	0.171 (0.56)
Incidence angle (chord line), deg	0
Leading-edge sweep, deg	50
V-tails:[a]	
Airfoil	NACA 4415
Rotor (reference):	
Radius, m (ft)	1.68 (5.50)
Disk area, m^2 (ft^2)	8.83 (95.0)

[a]See figure 4 and Symbols for details.

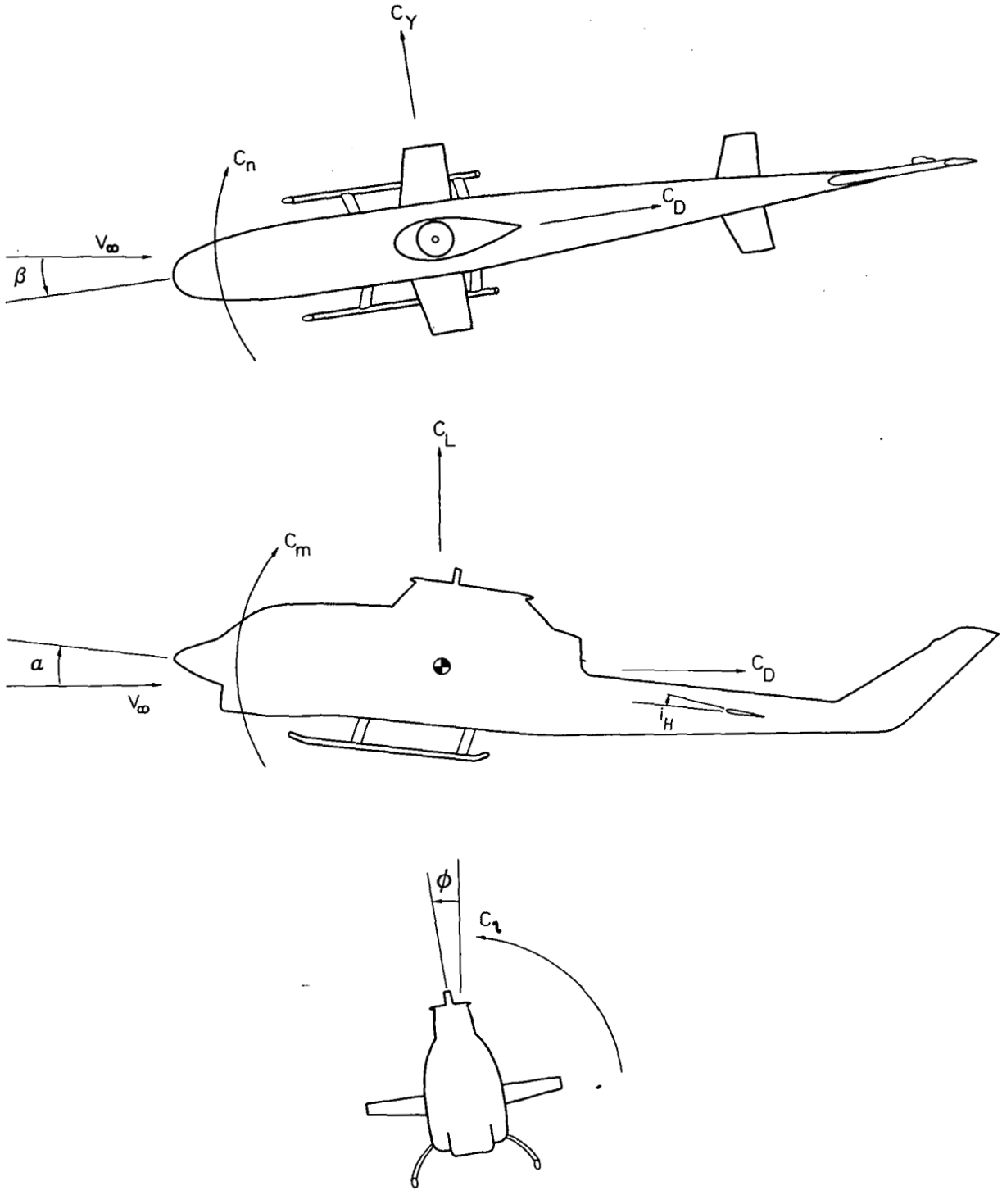

Figure 1.- Axes and sign conventions. Positive directions are indicated by arrows.

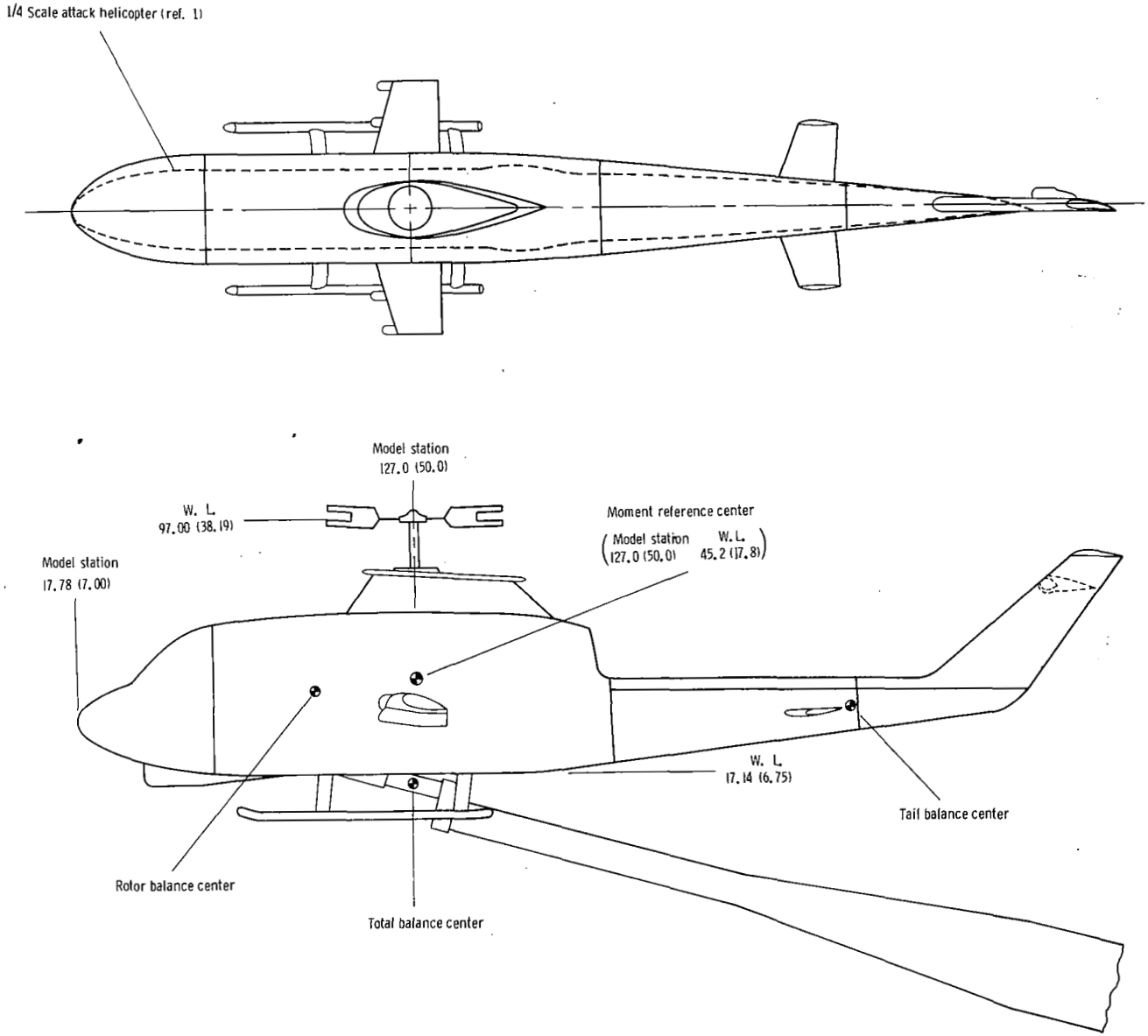

Figure 2.- Model geometry. Dimensions are in cm (in.).

L-76-3552

Figure 3.- Model with small V-tail.

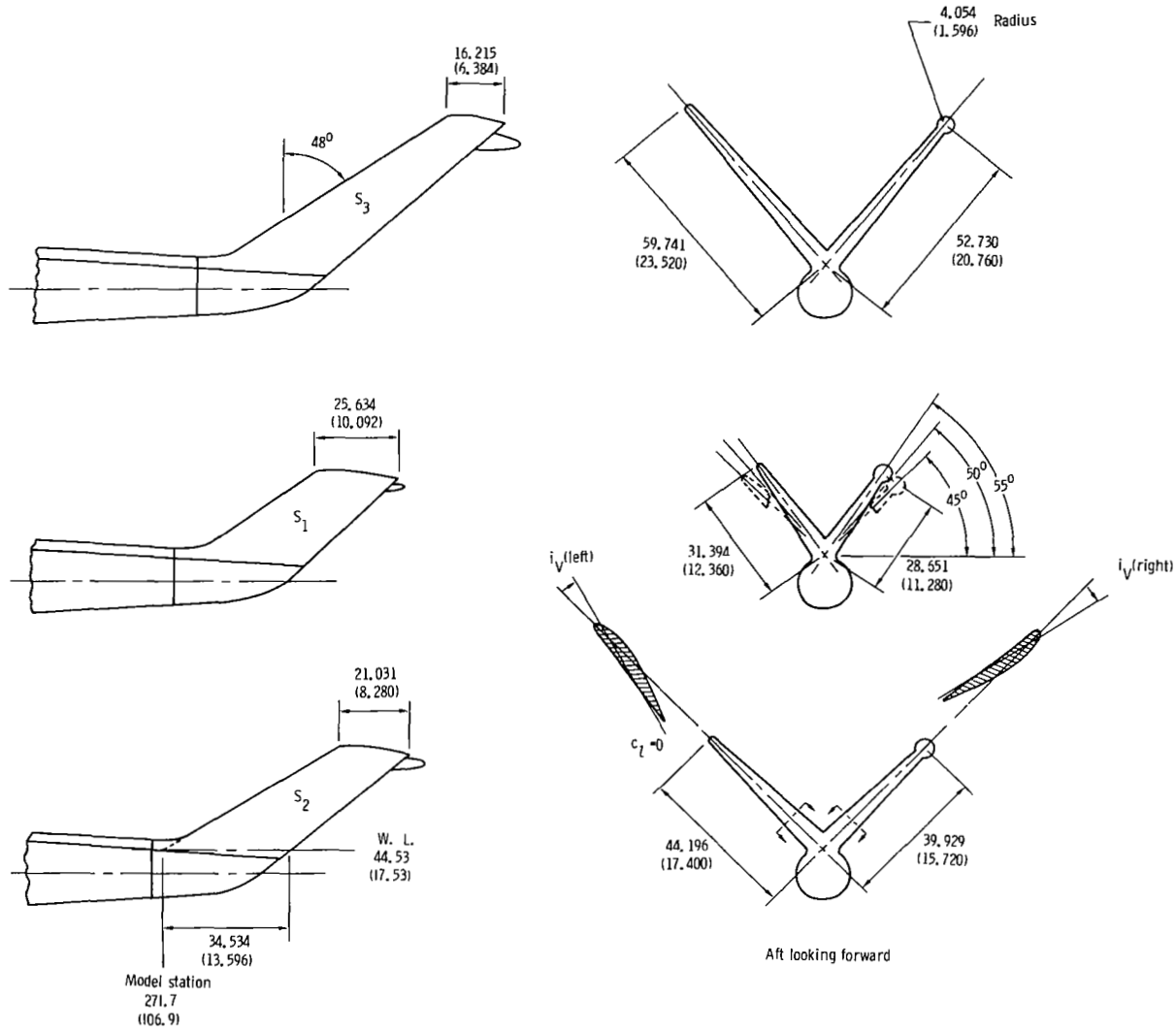

Figure 4.- V-tail geometry. Dimensions are in cm (in.).

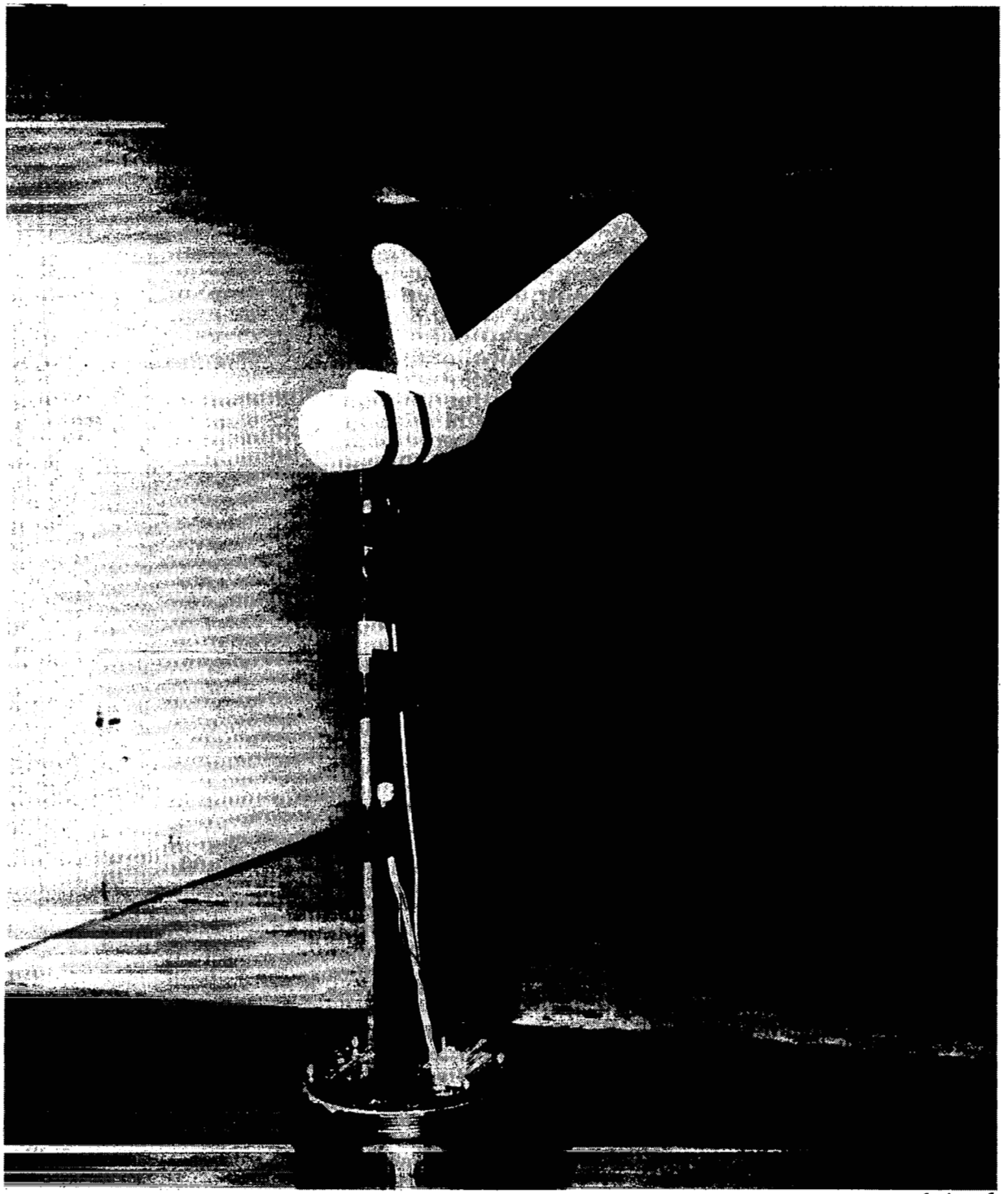

L-76-4116

Figure 5.- V-tail without fuselage.

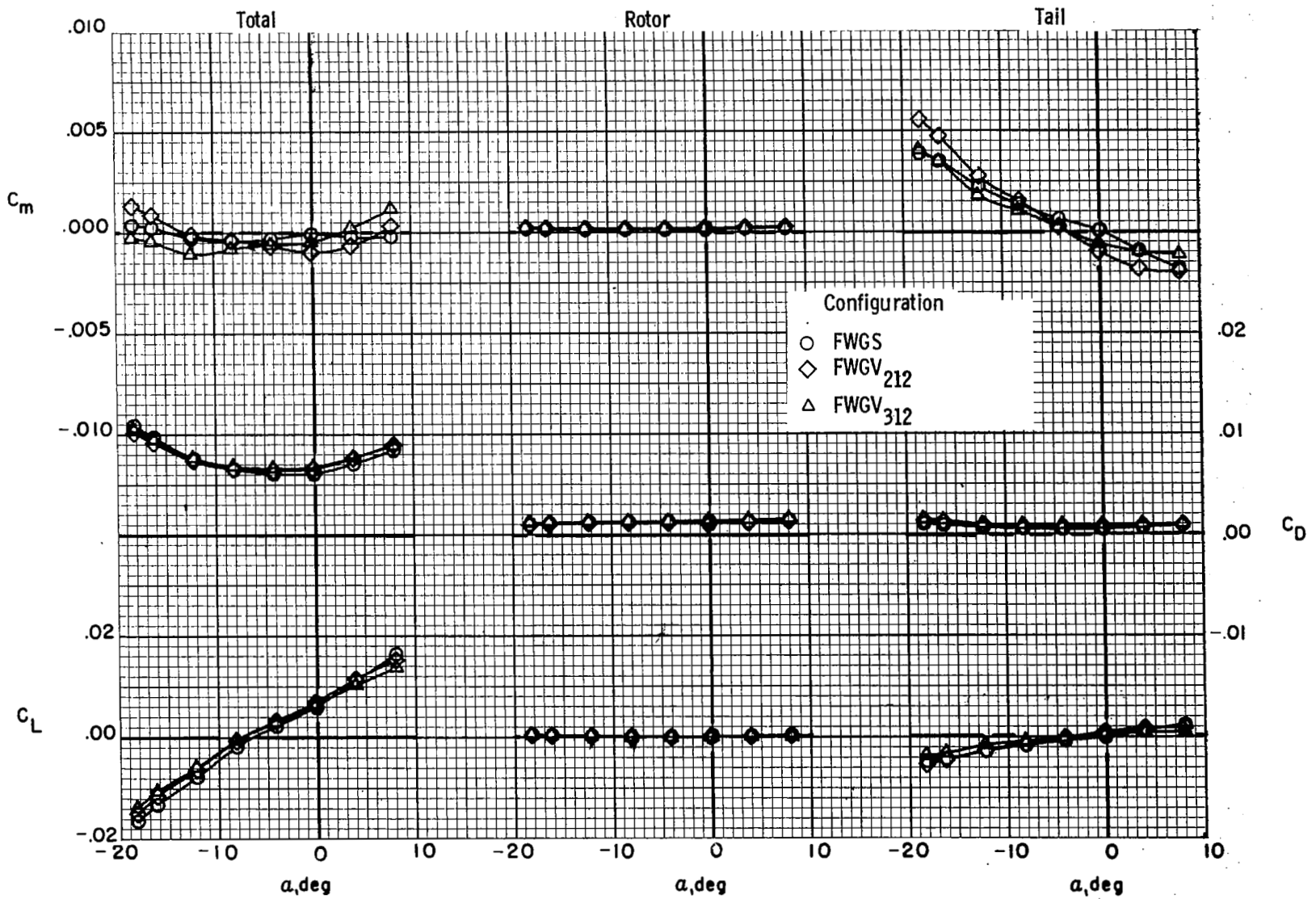

(a) S_1; $i_V = 8^o$.

Figure 6.- Effect of V-tail dihedral angle on model longitudinal characteristics.

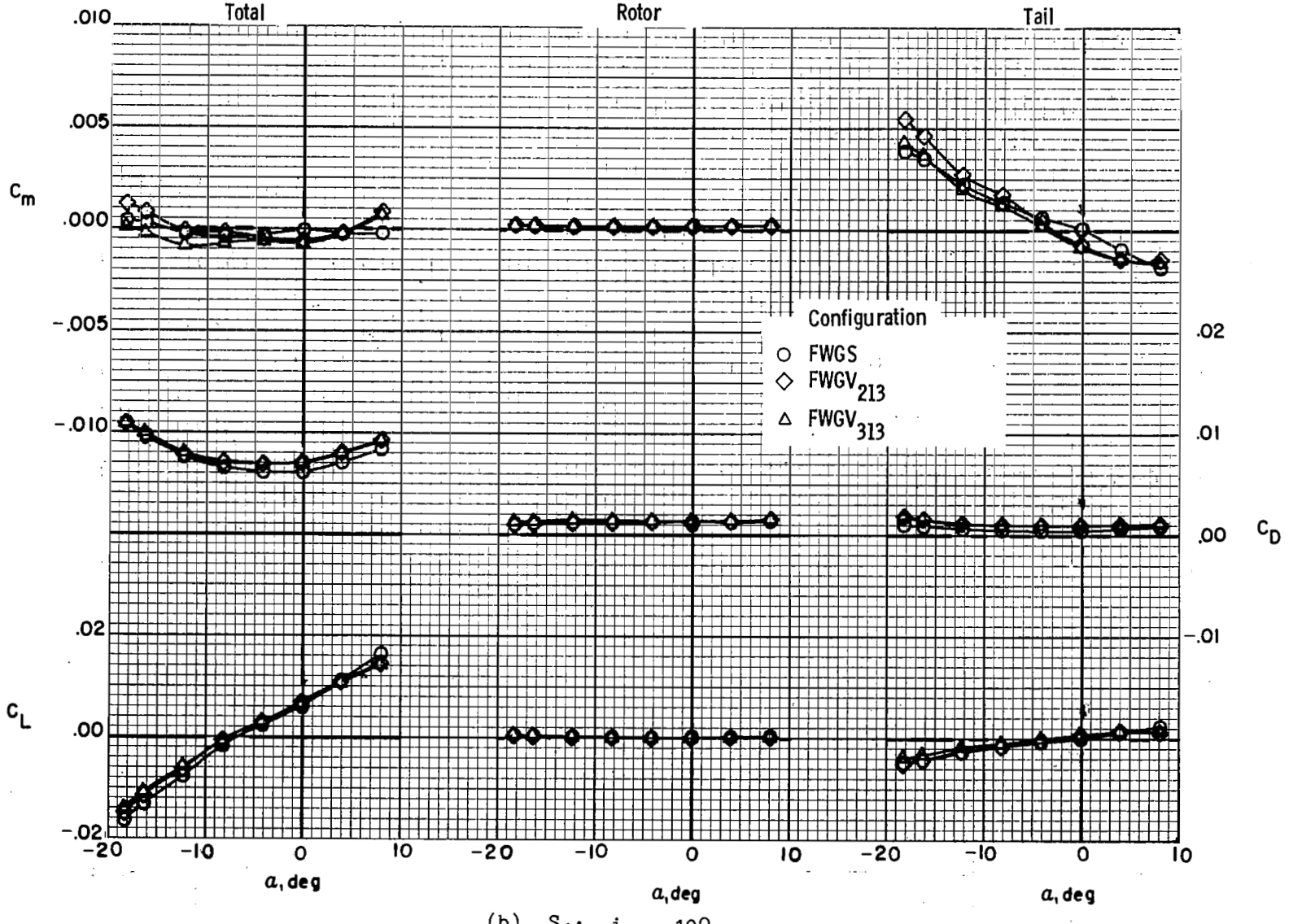

(b) S_1; $i_V = 10^o$.

Figure 6.- Continued.

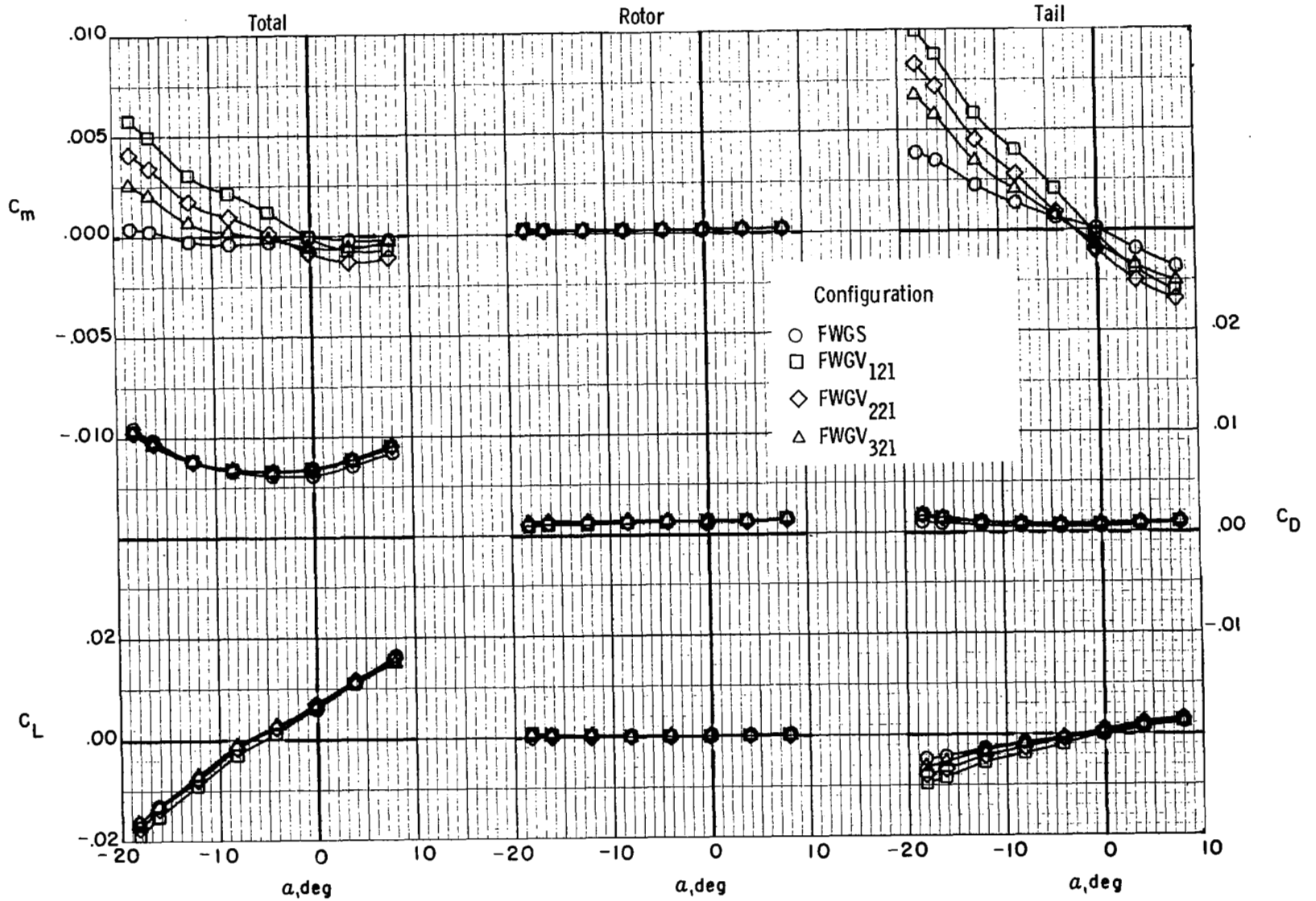

(c) S_2; $i_V = 5^o$.

Figure 6.- Continued.

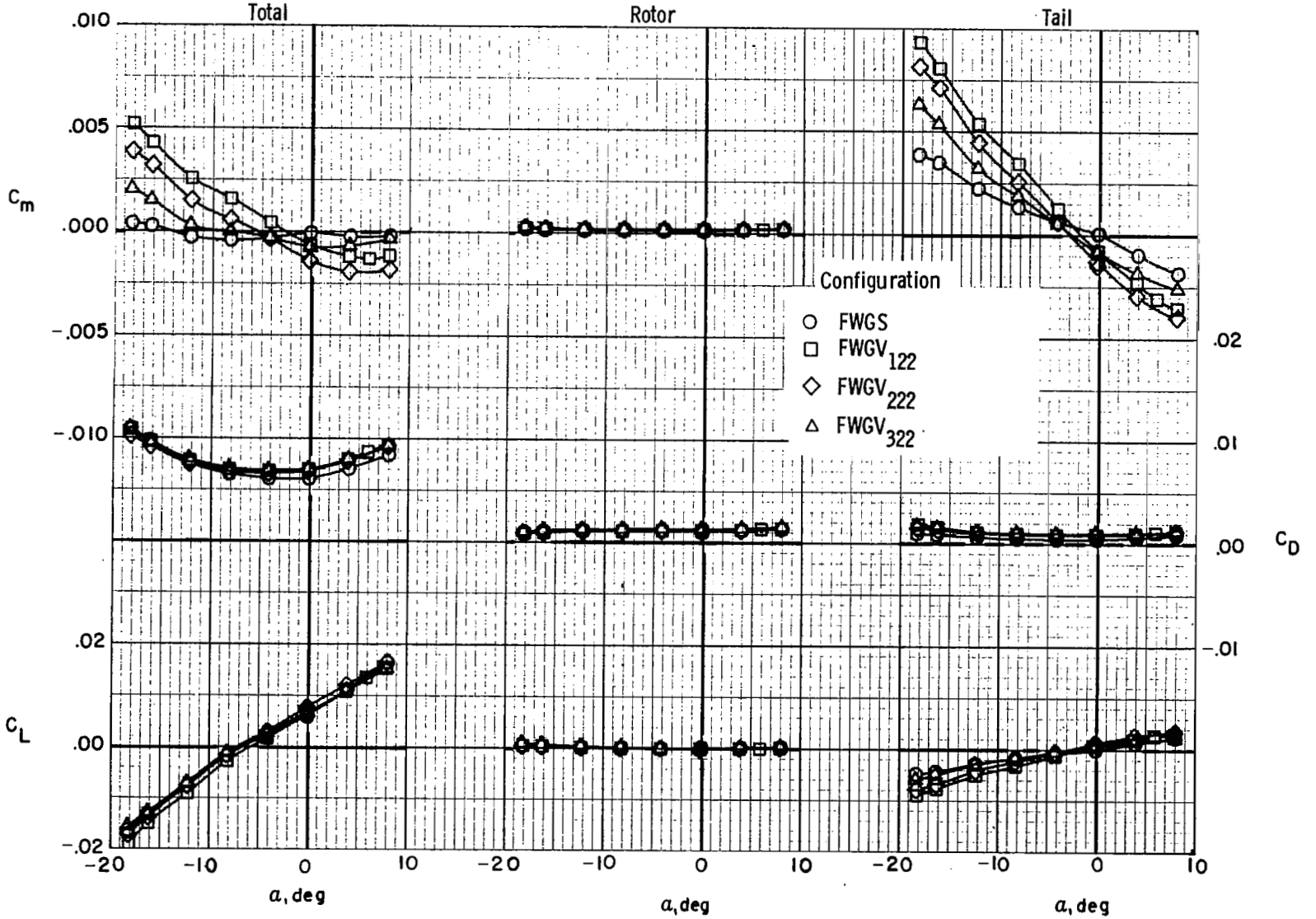

(d) S_2; $i_V = 8^o$.

Figure 6.- Continued.

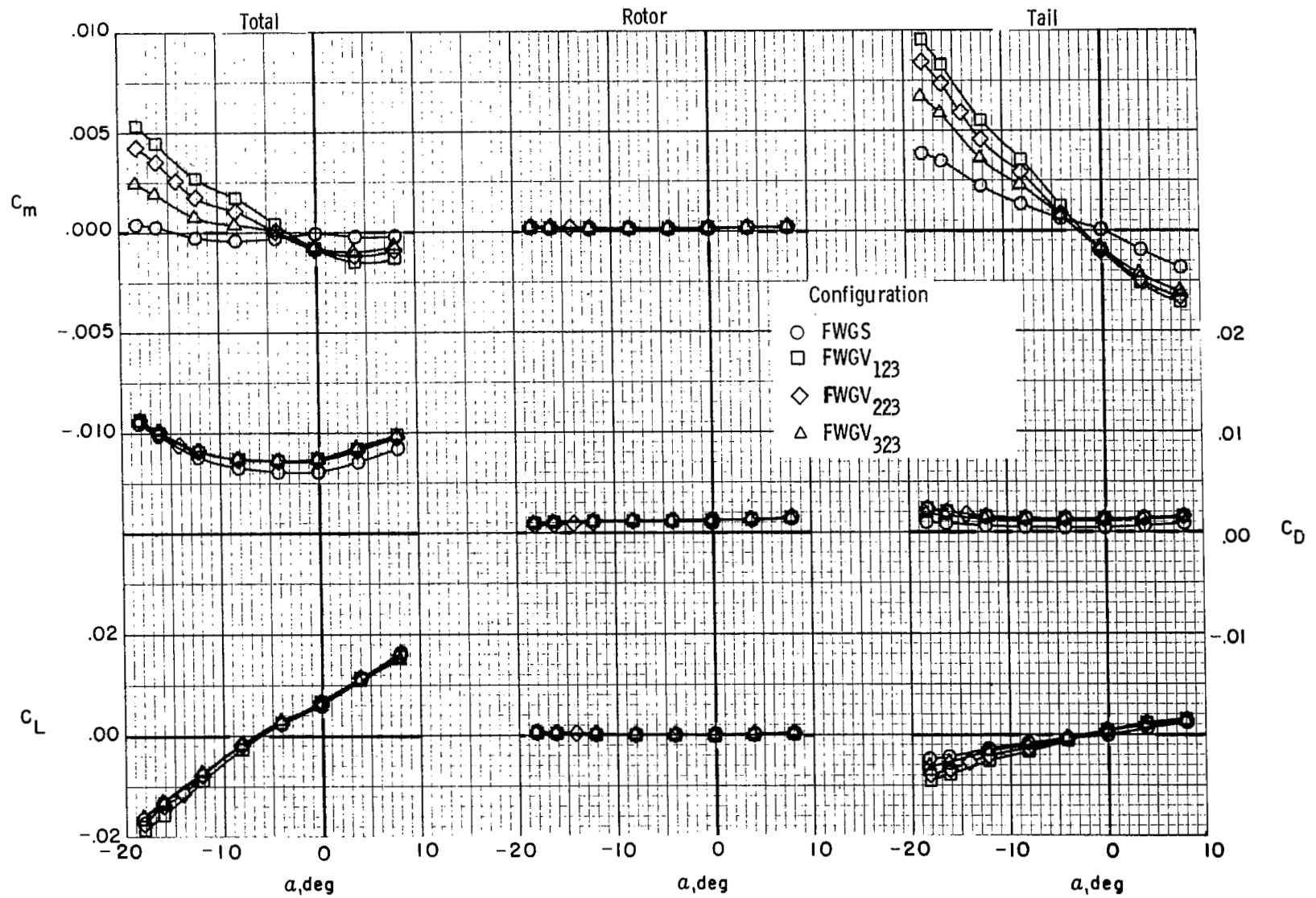

(e) S_2; $i_V = 10^o$.

Figure 6.- Concluded.

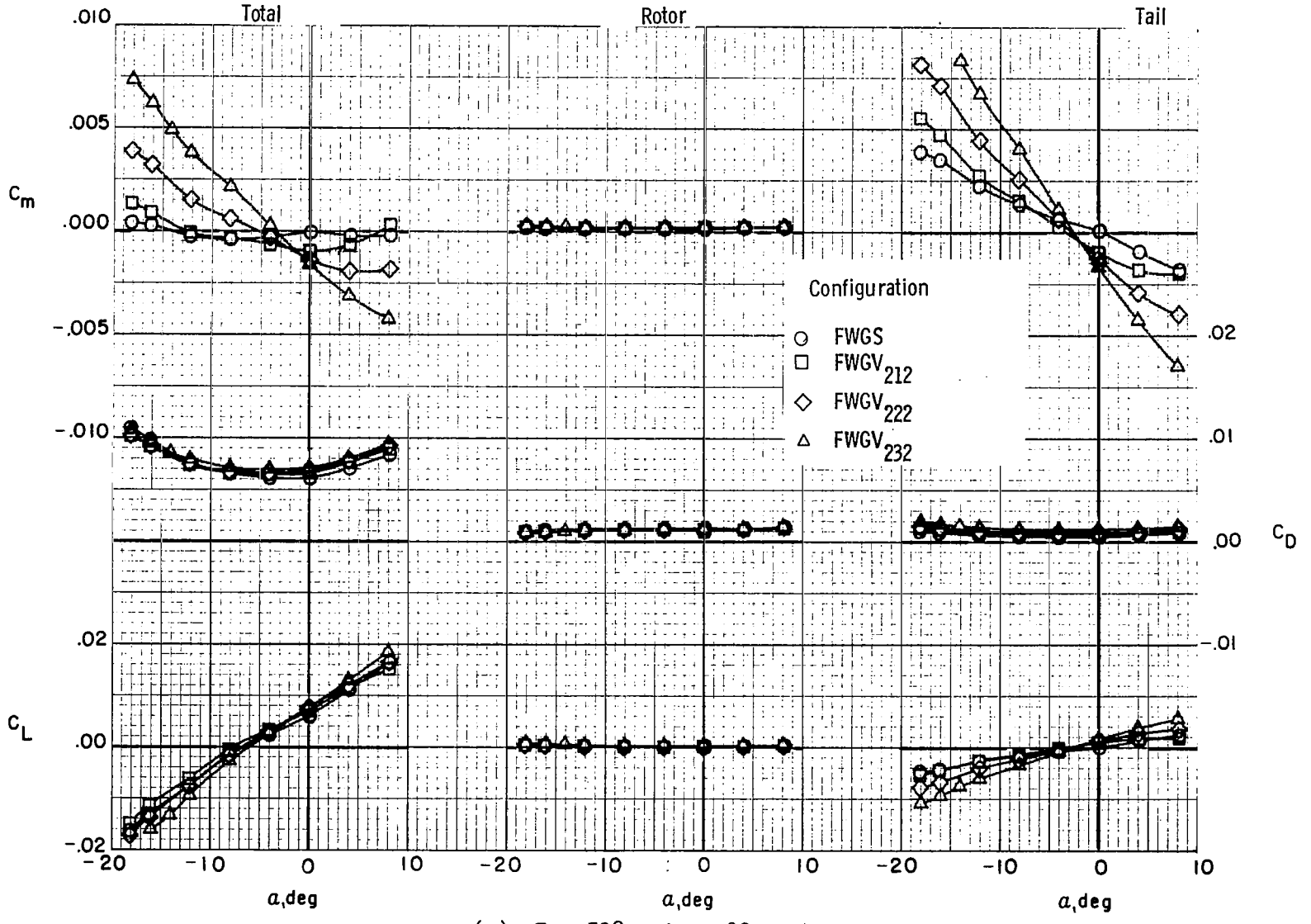

(a) $\Gamma = 50^{\circ}$; $i_V = 8^{\circ}$.

Figure 7.- Effect of V-tail planform area on model longitudinal characteristics.

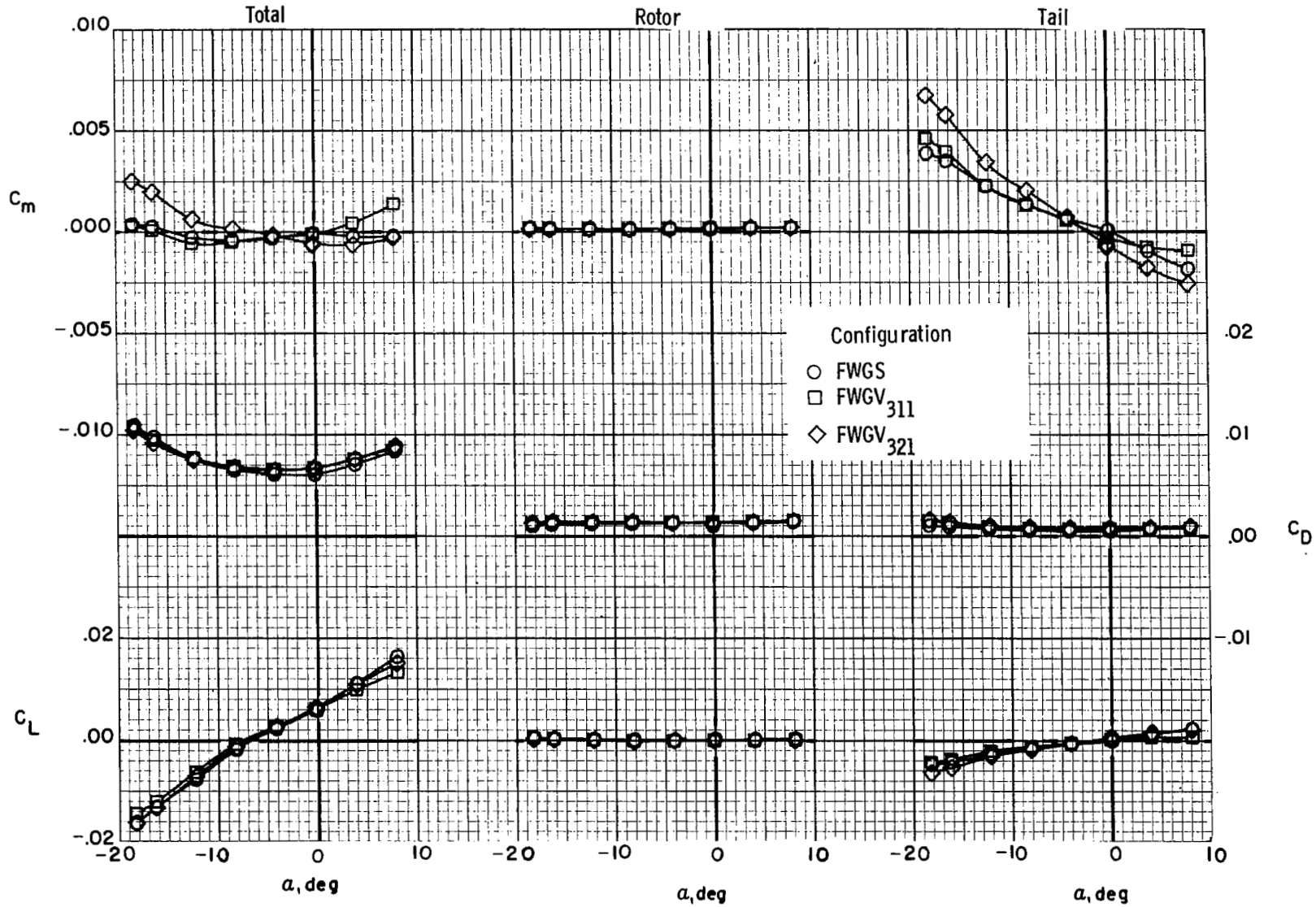

(b) $\Gamma = 55^{\circ}$; $i_V = 5^{\circ}$.

Figure 7.- Continued.

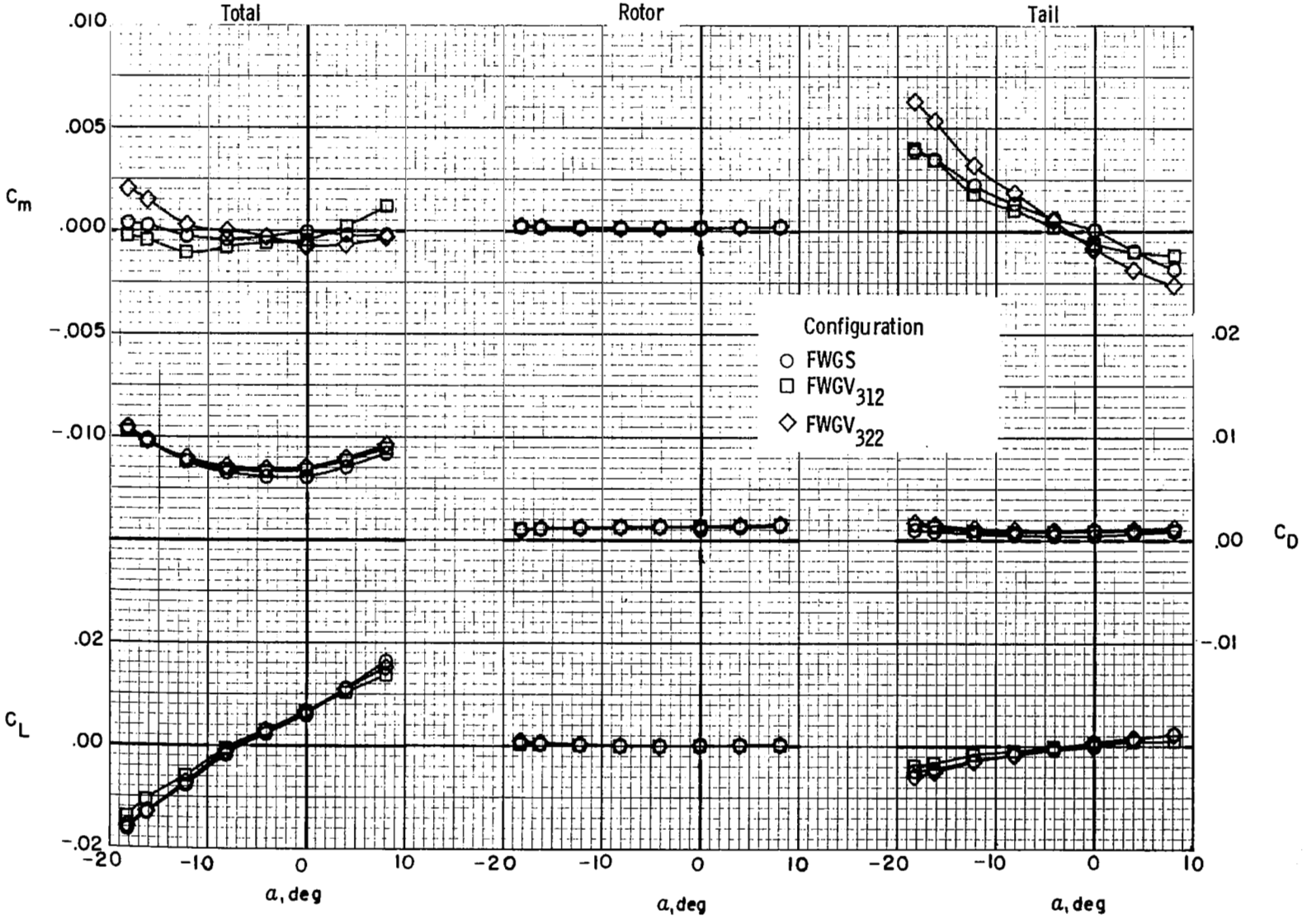

(c) $\Gamma = 55^{\circ}$; $i_V = 8^{\circ}$.

Figure 7.- Continued.

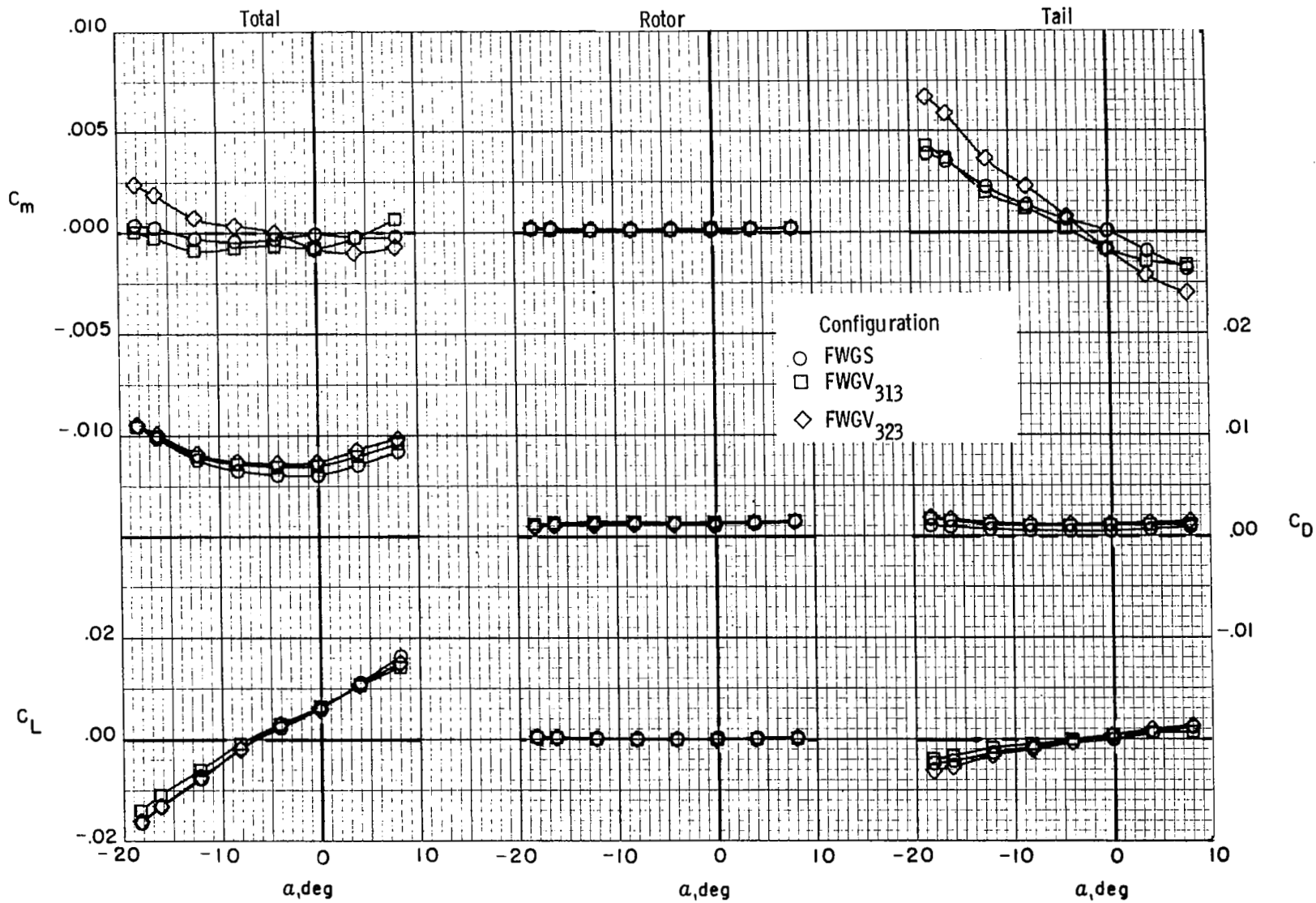

(d) $\Gamma = 55^{\circ}$; $i_V = 10^{\circ}$.

Figure 7.- Concluded.

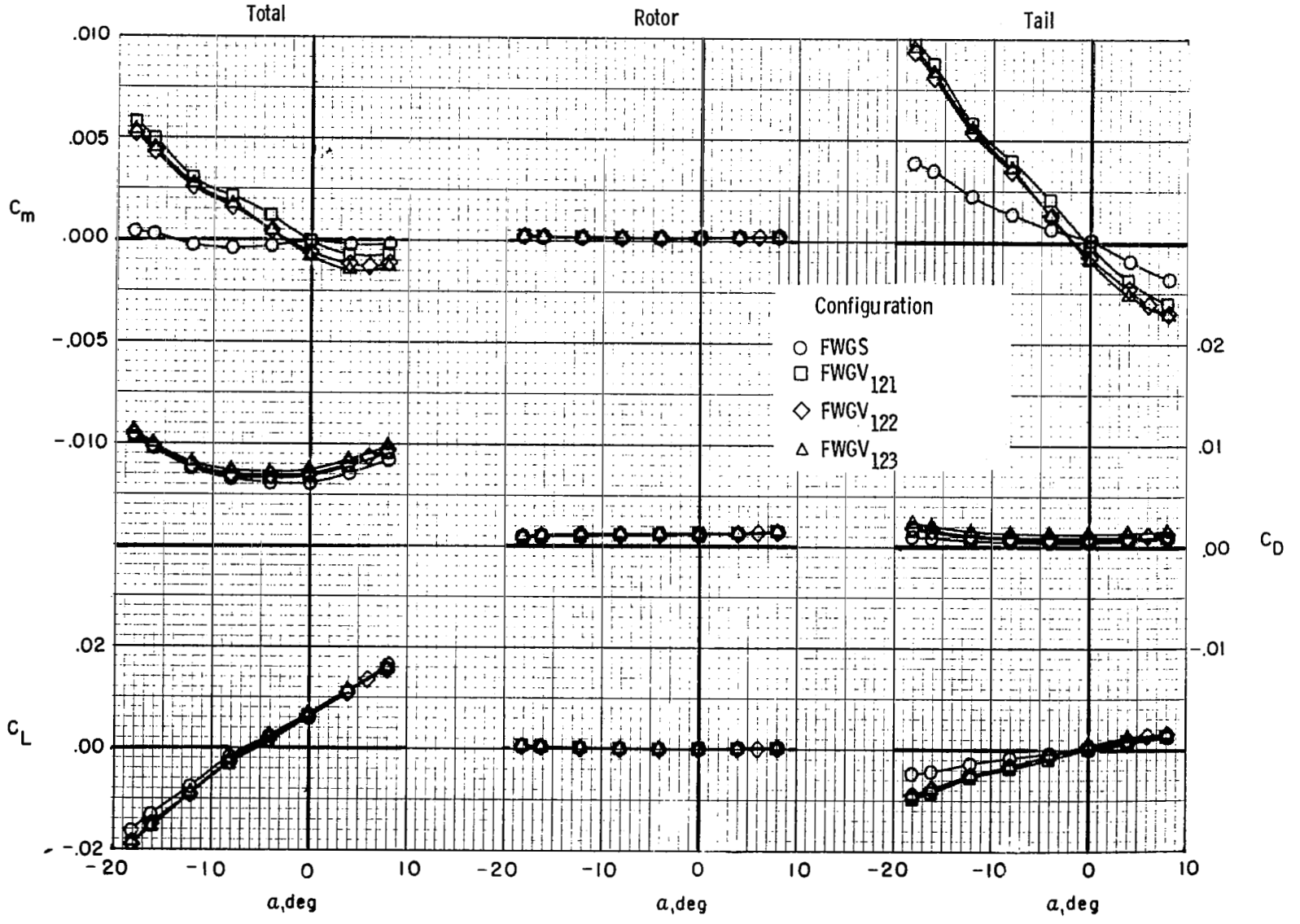

(a) $\Gamma = 45^{\circ}$; S_2.

Figure 8.- Effect of V-tail incidence angle on model longitudinal characteristics.

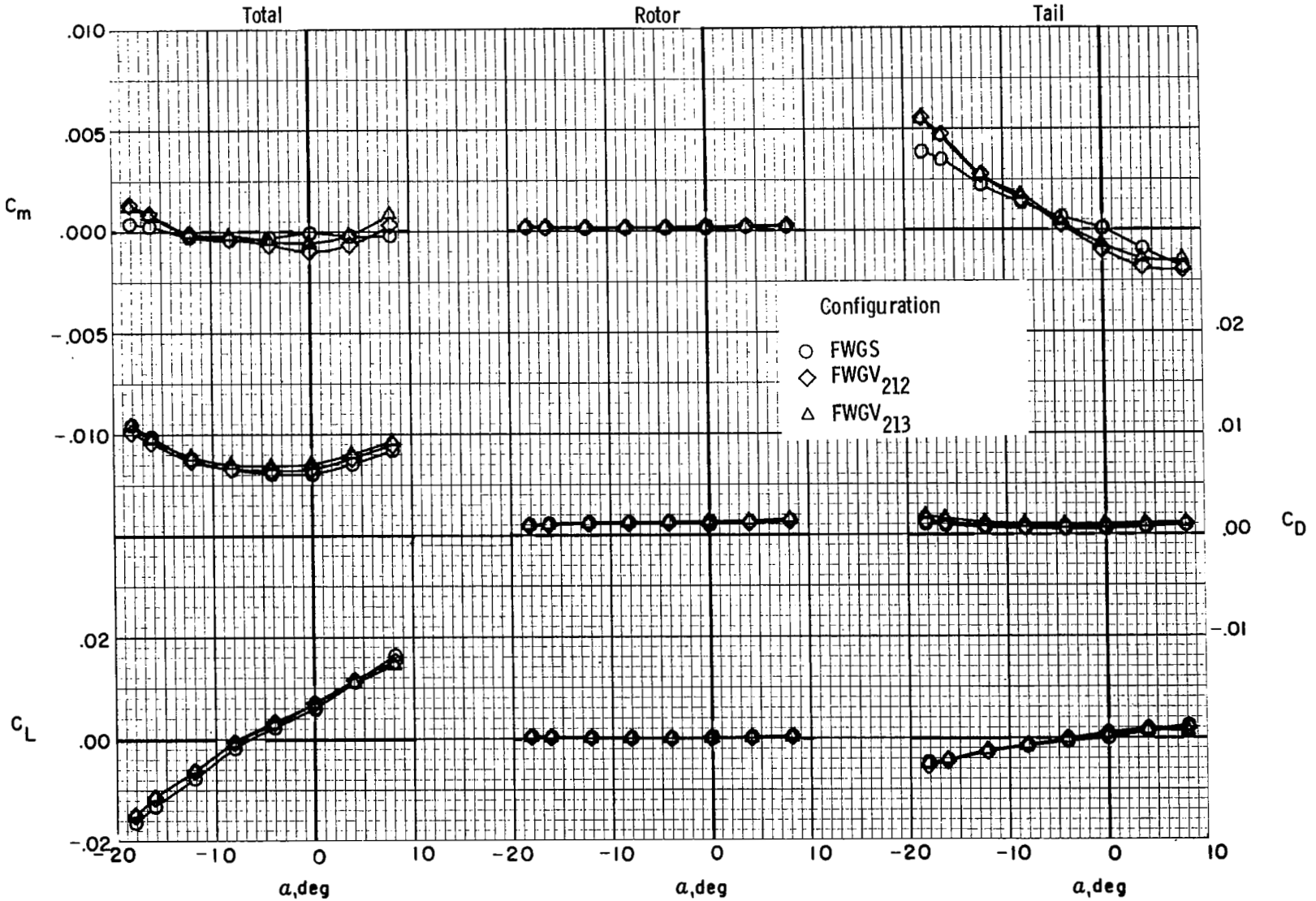

(b) $\Gamma = 50^{\circ}$; S_1.

Figure 8.- Continued.

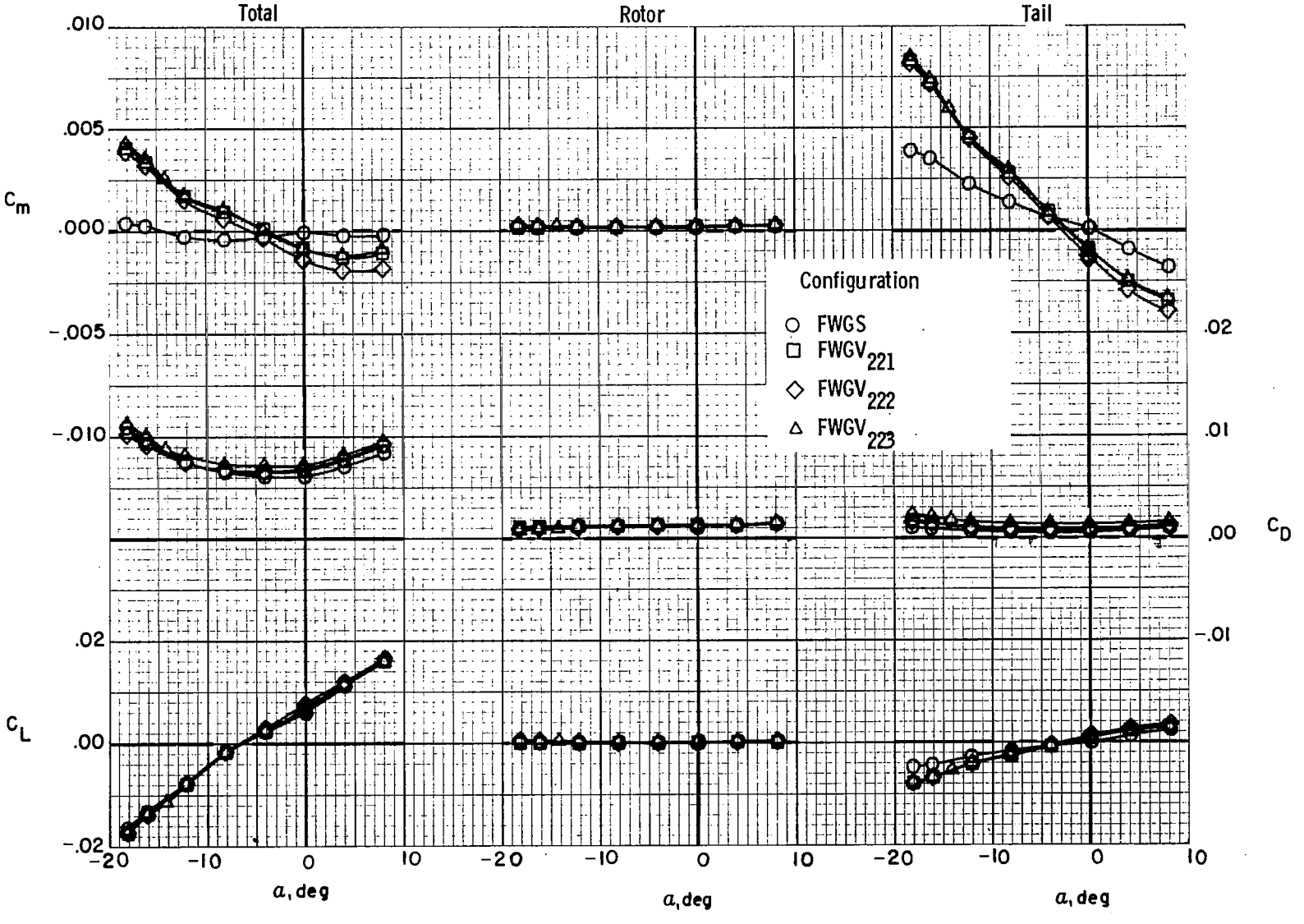

(c) $\Gamma = 50^{\circ}$; S_2.

Figure 8.- Continued.

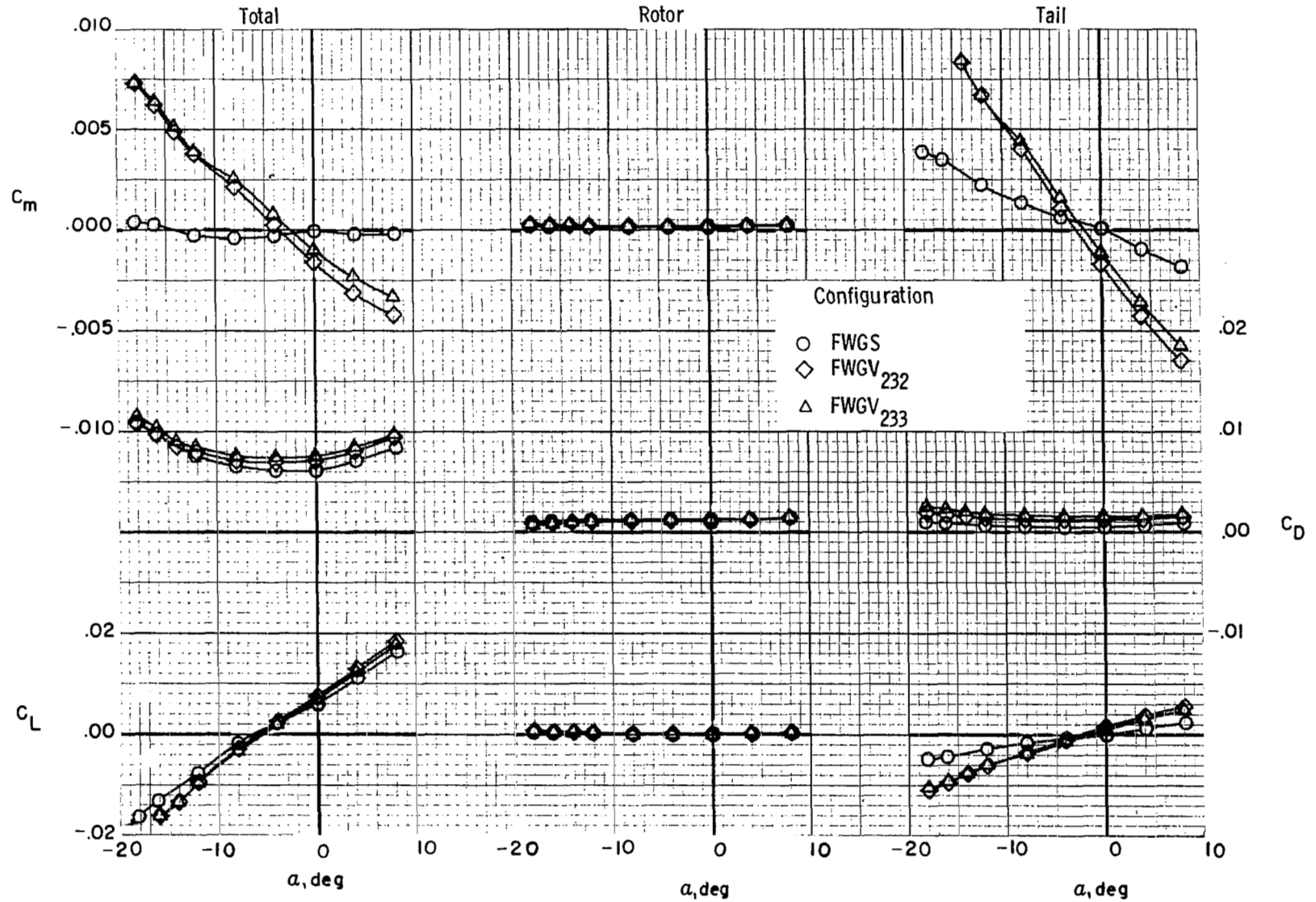

(d) $\Gamma = 55^{\circ}$; S_3.

Figure 8.- Continued.

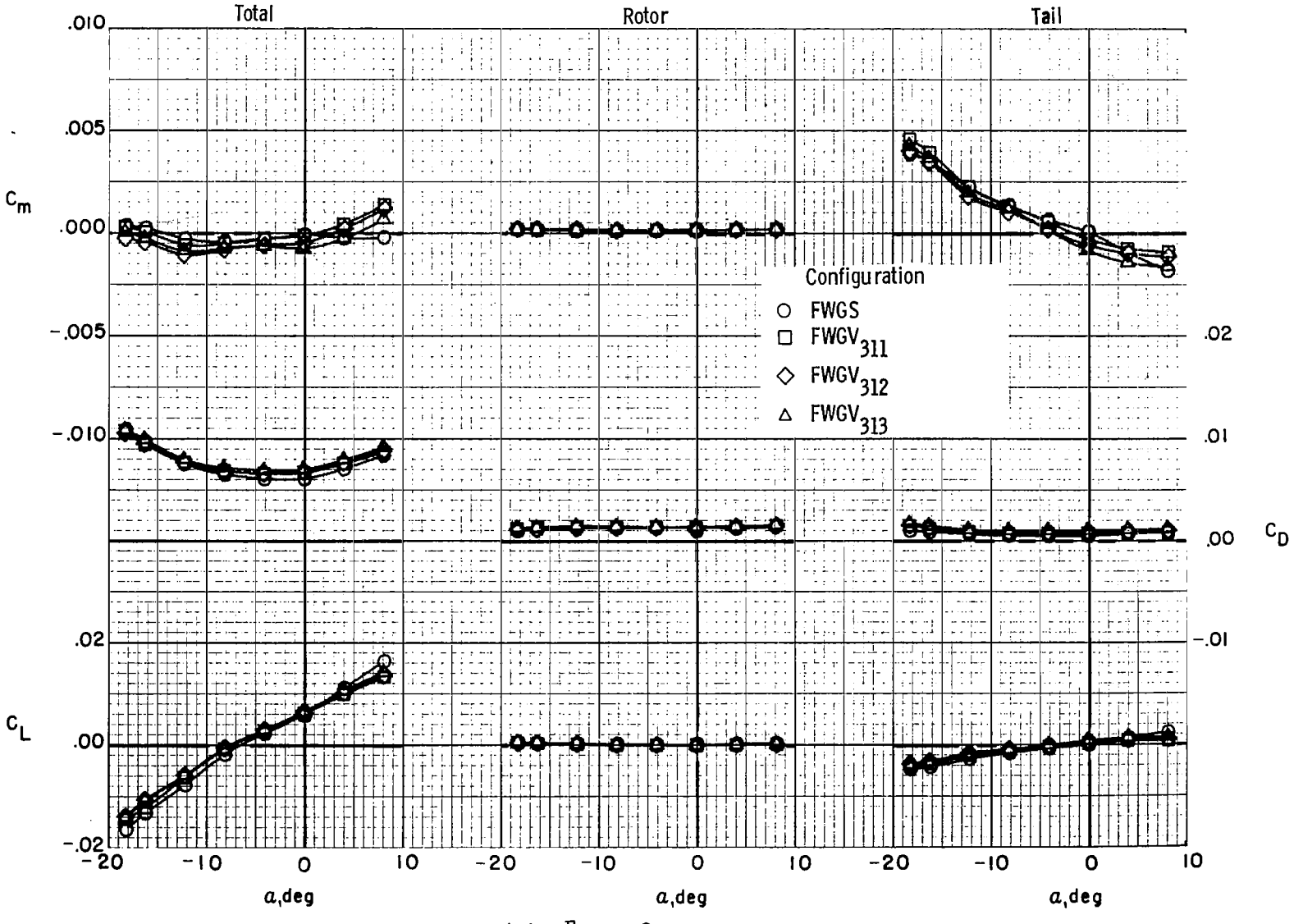

(e) $\Gamma = 55^{\circ}$; S_1.

Figure 8.- Continued.

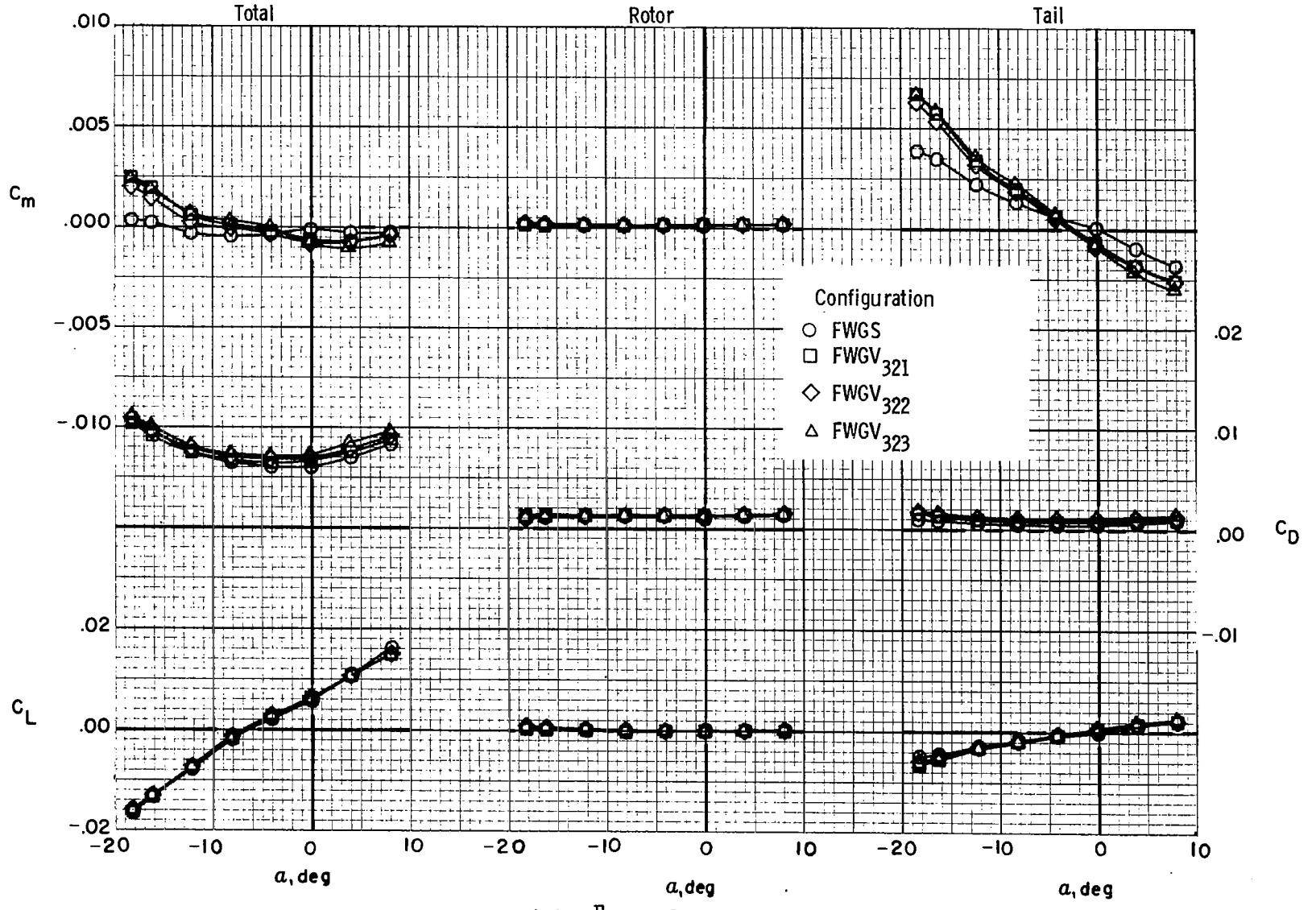

(f) $\Gamma = 55^{\circ}$; S_2.

Figure 8.- Concluded.

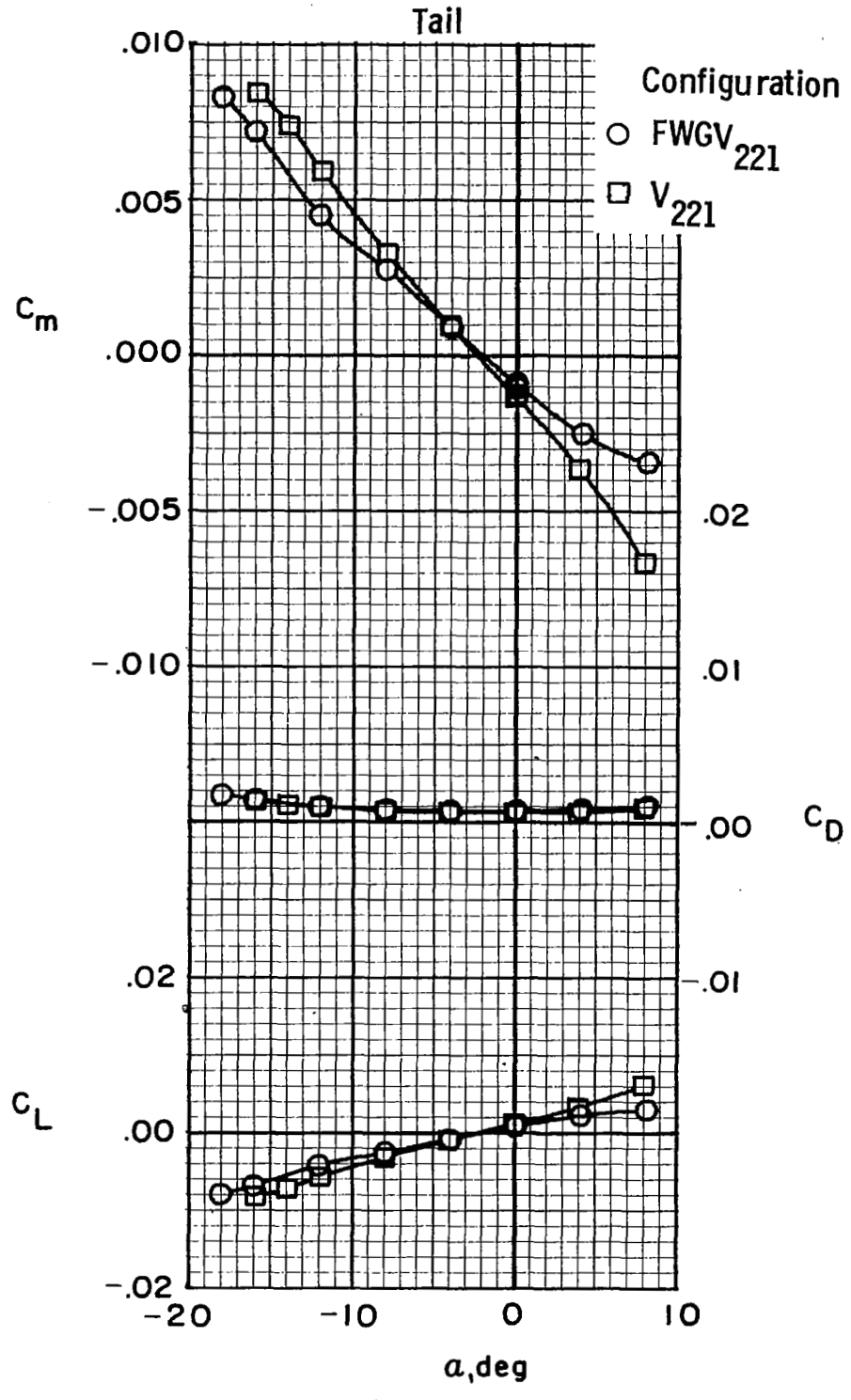

(a) V_{221}.

Figure 9.- Effect of fuselage on model longitudinal characteristics.

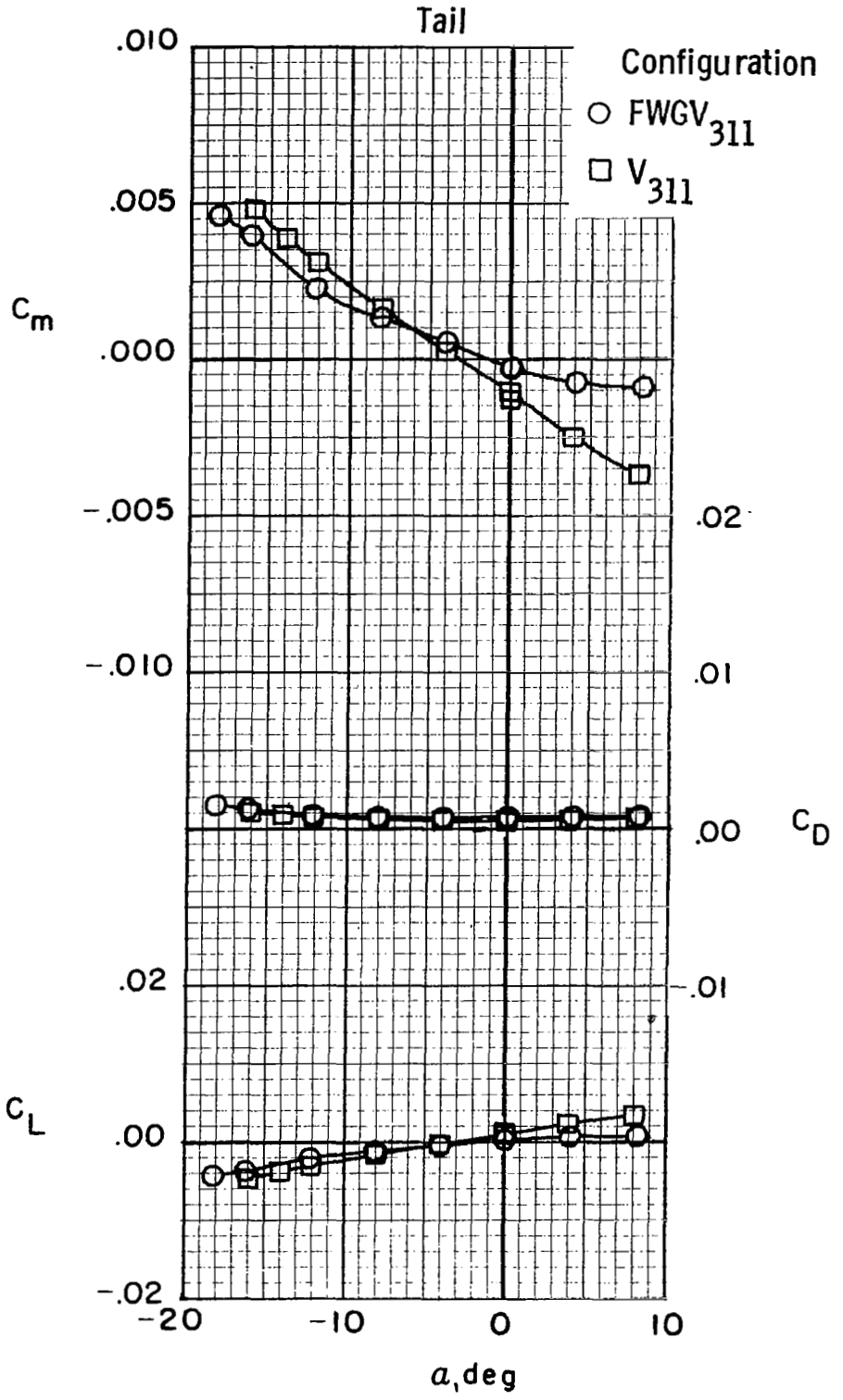

(b) V_{311}.

Figure 9.- Continued.

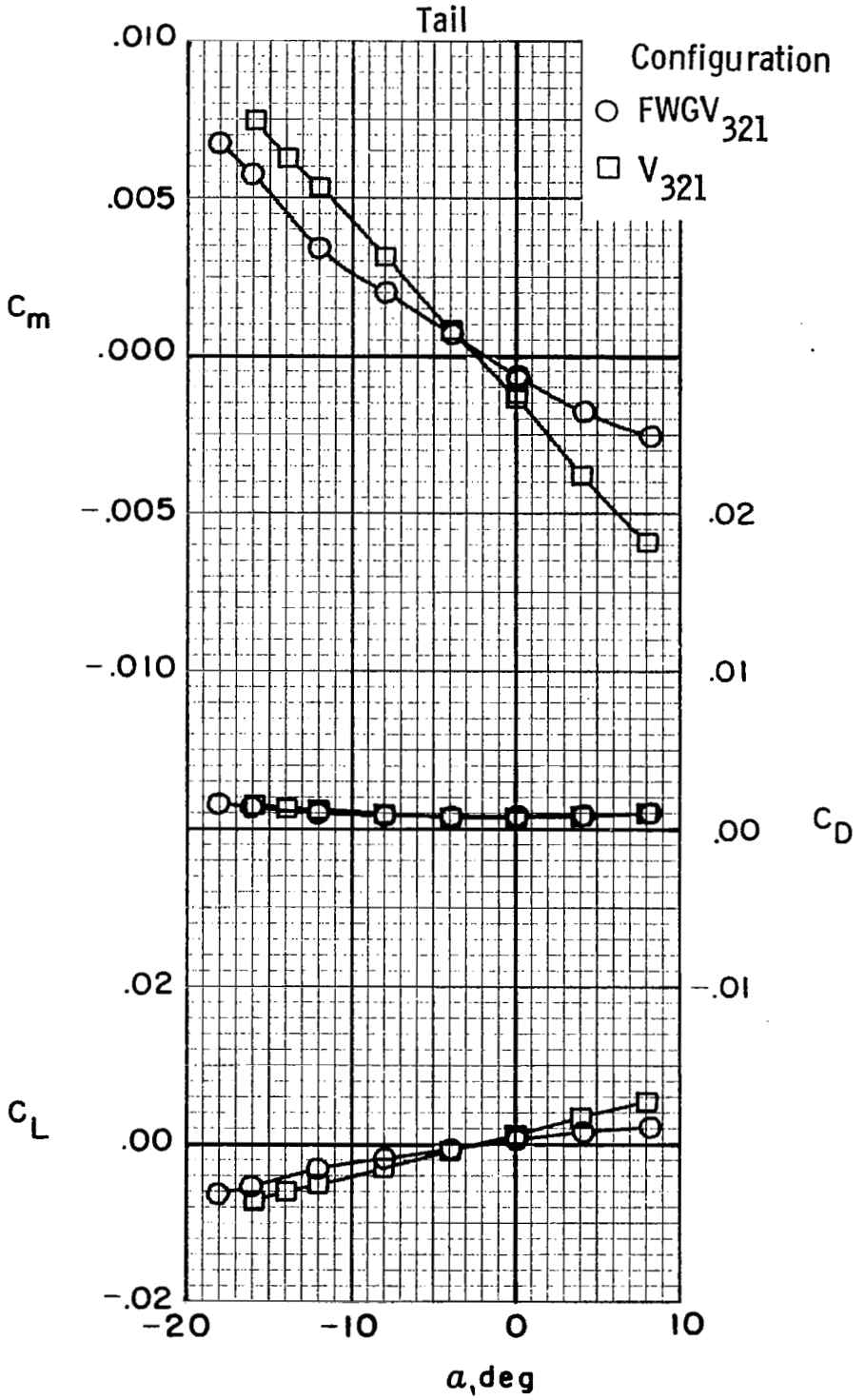

(c) V_{321}.

Figure 9.- Concluded.

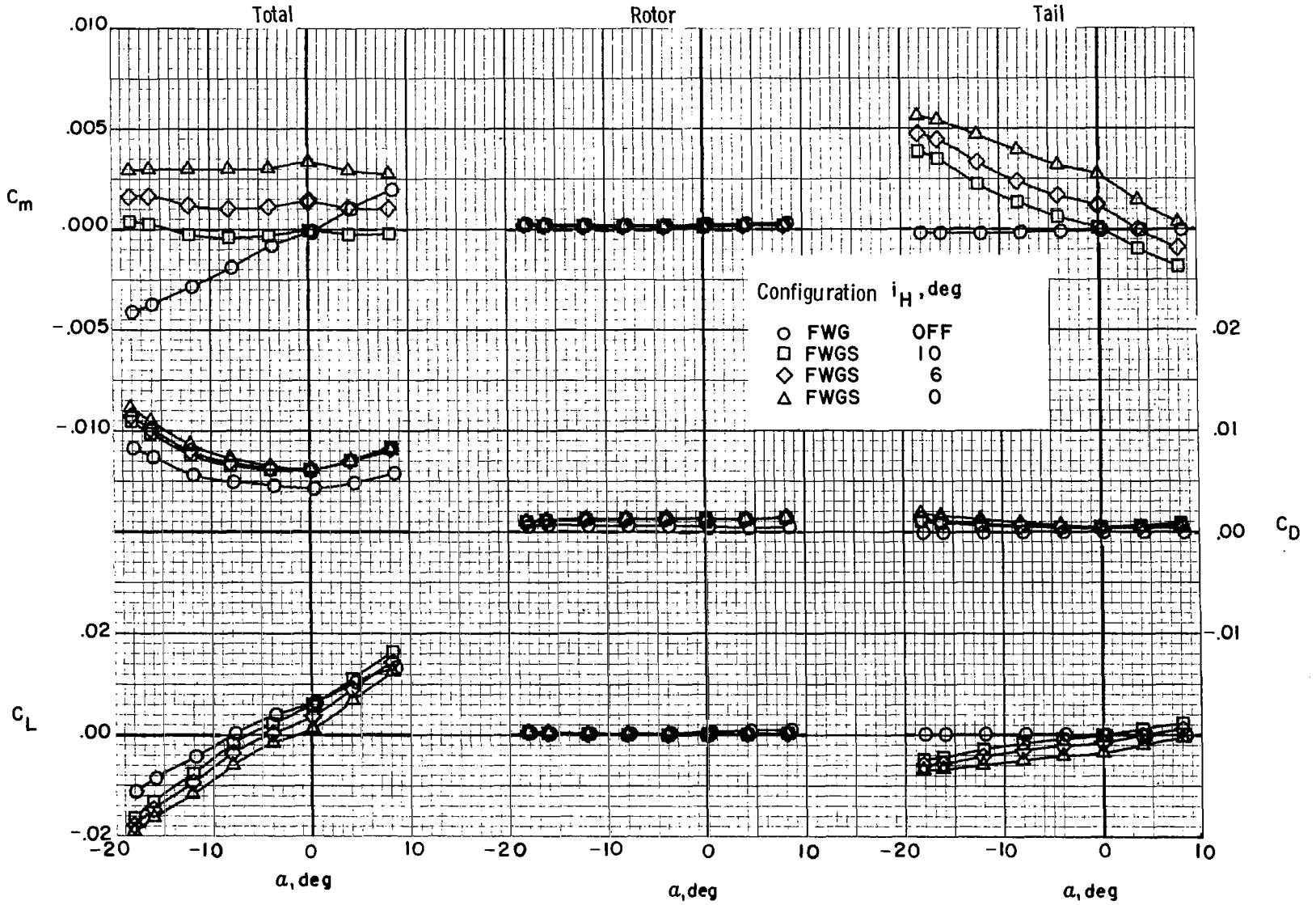

Figure 10.- Effect of horizontal-tail incidence angle on model longitudinal characteristics.

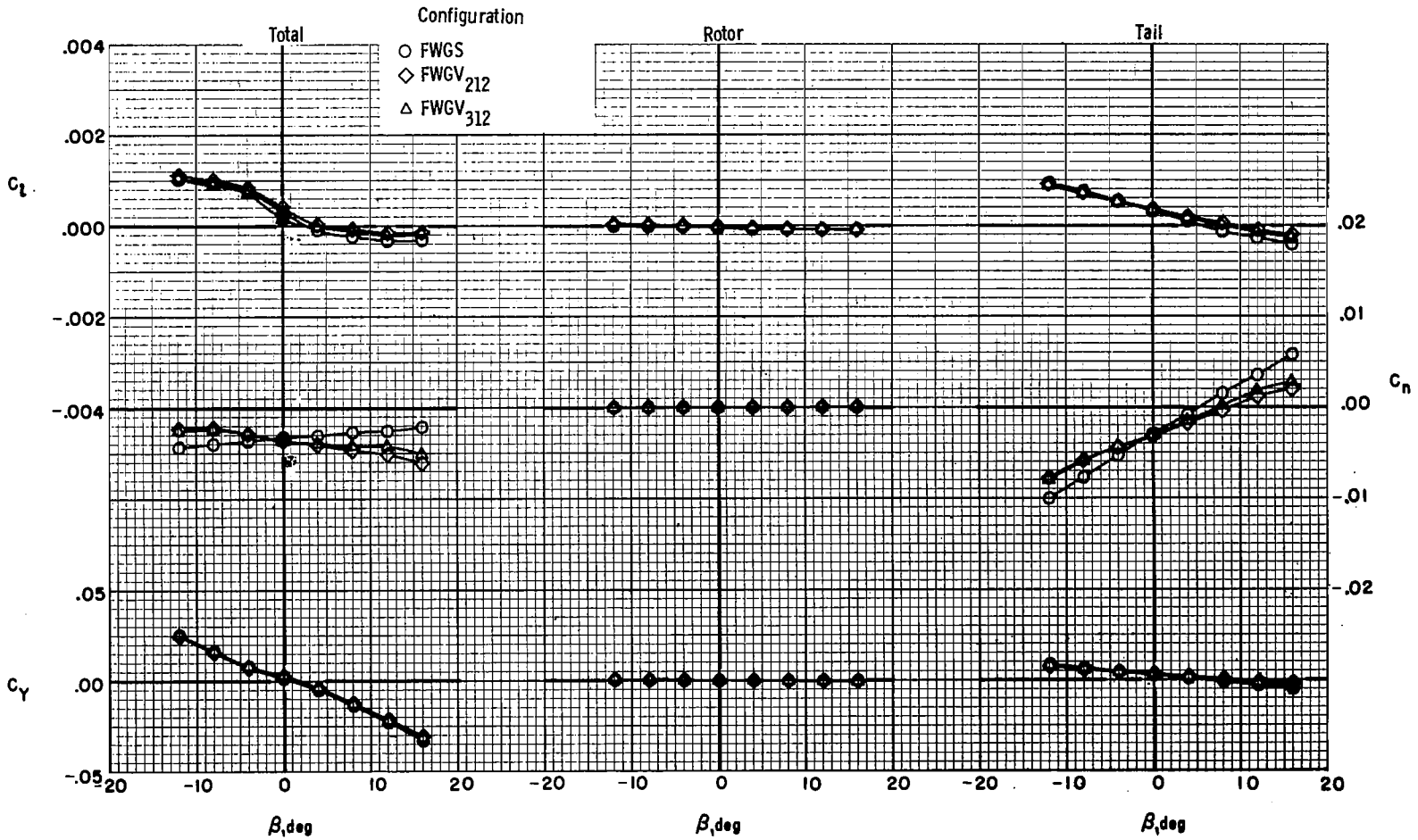

(a) S_1; $i_V = 8^o$.

Figure 11.- Effect of V-tail dihedral angle on model lateral-directional characteristics.

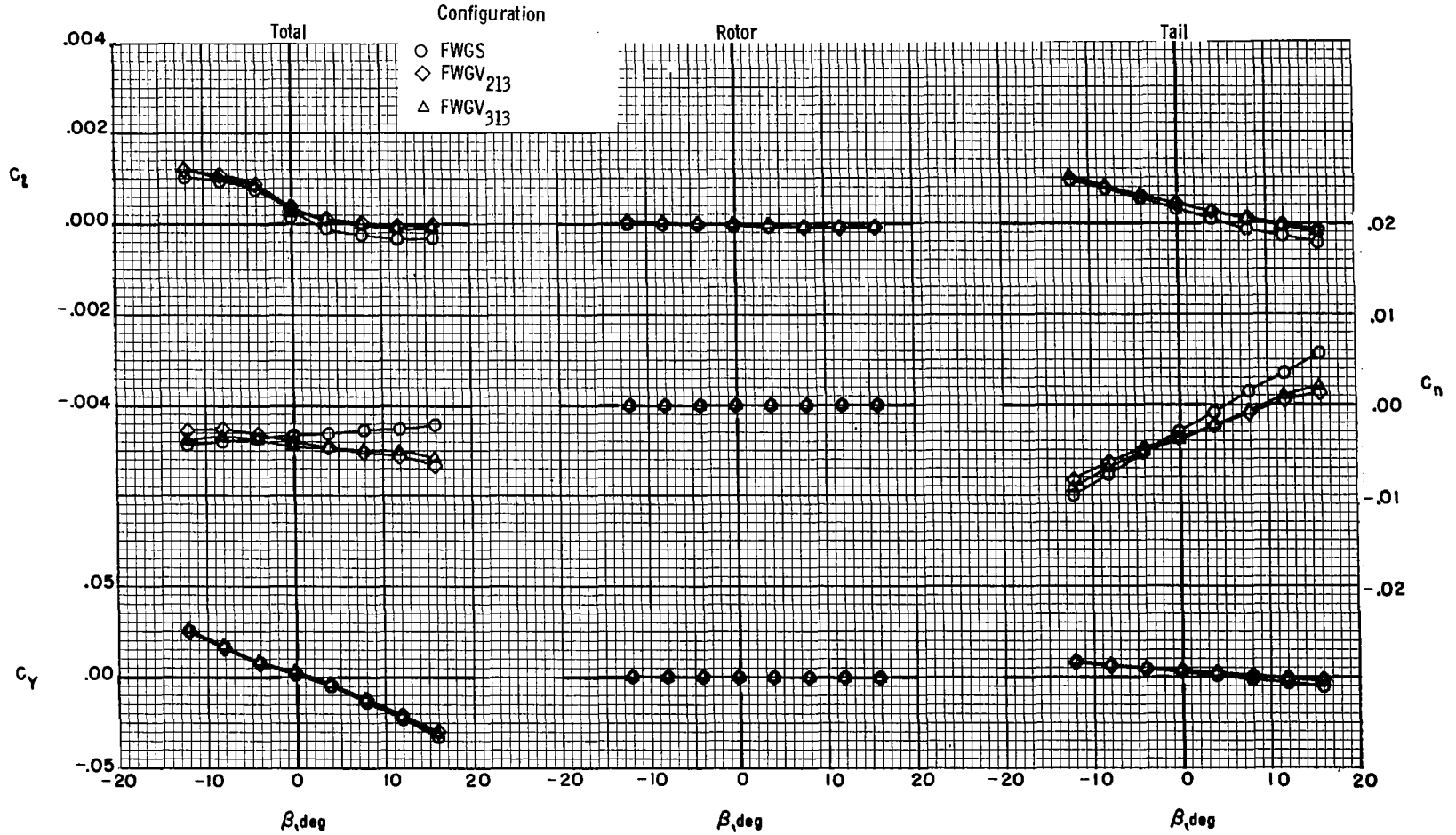

(b) S_1; $i_V = 10^o$.

Figure 11.- Continued.

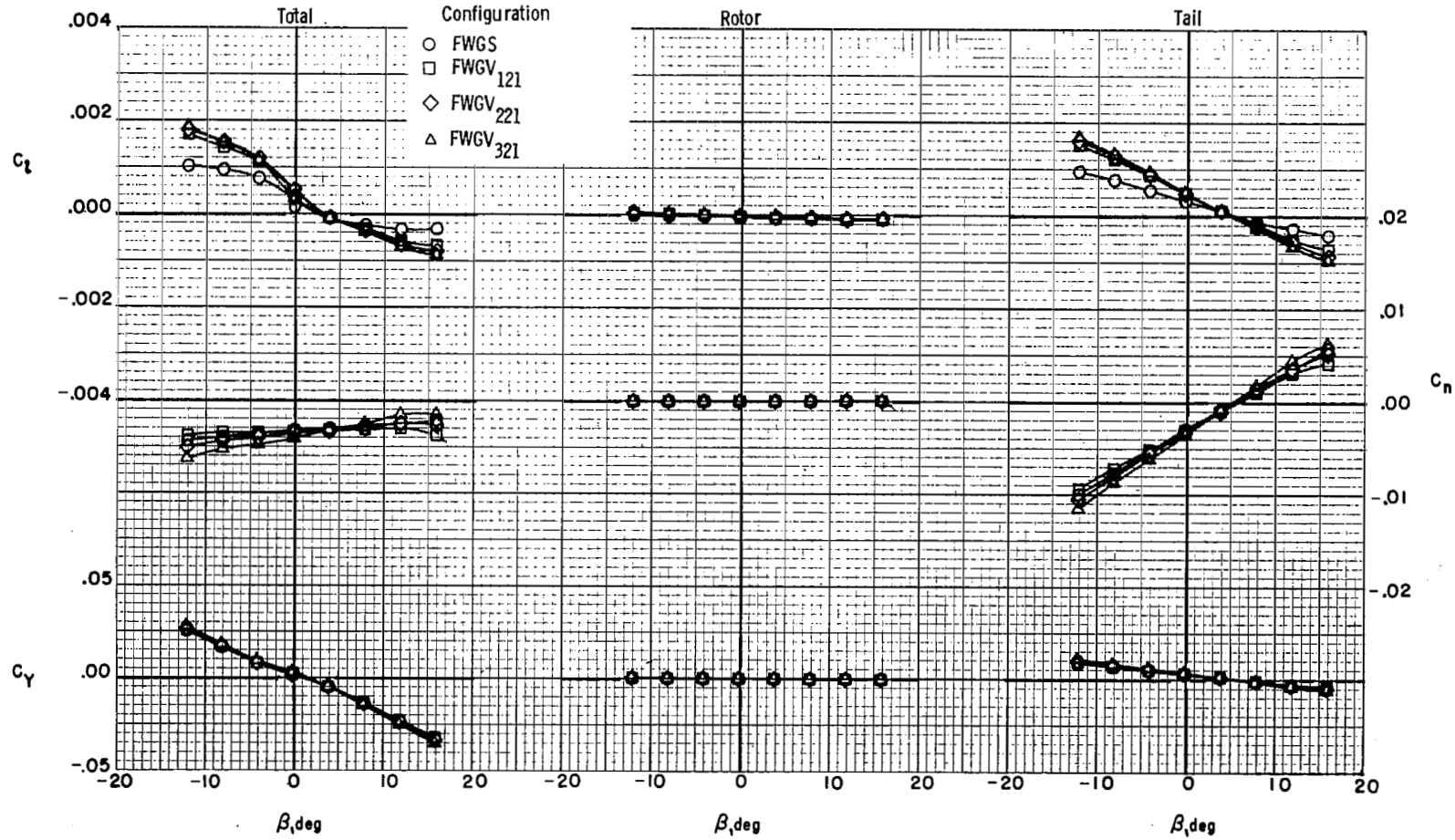

(c) S_2; $i_V = 5^\circ$.

Figure 11.- Continued.

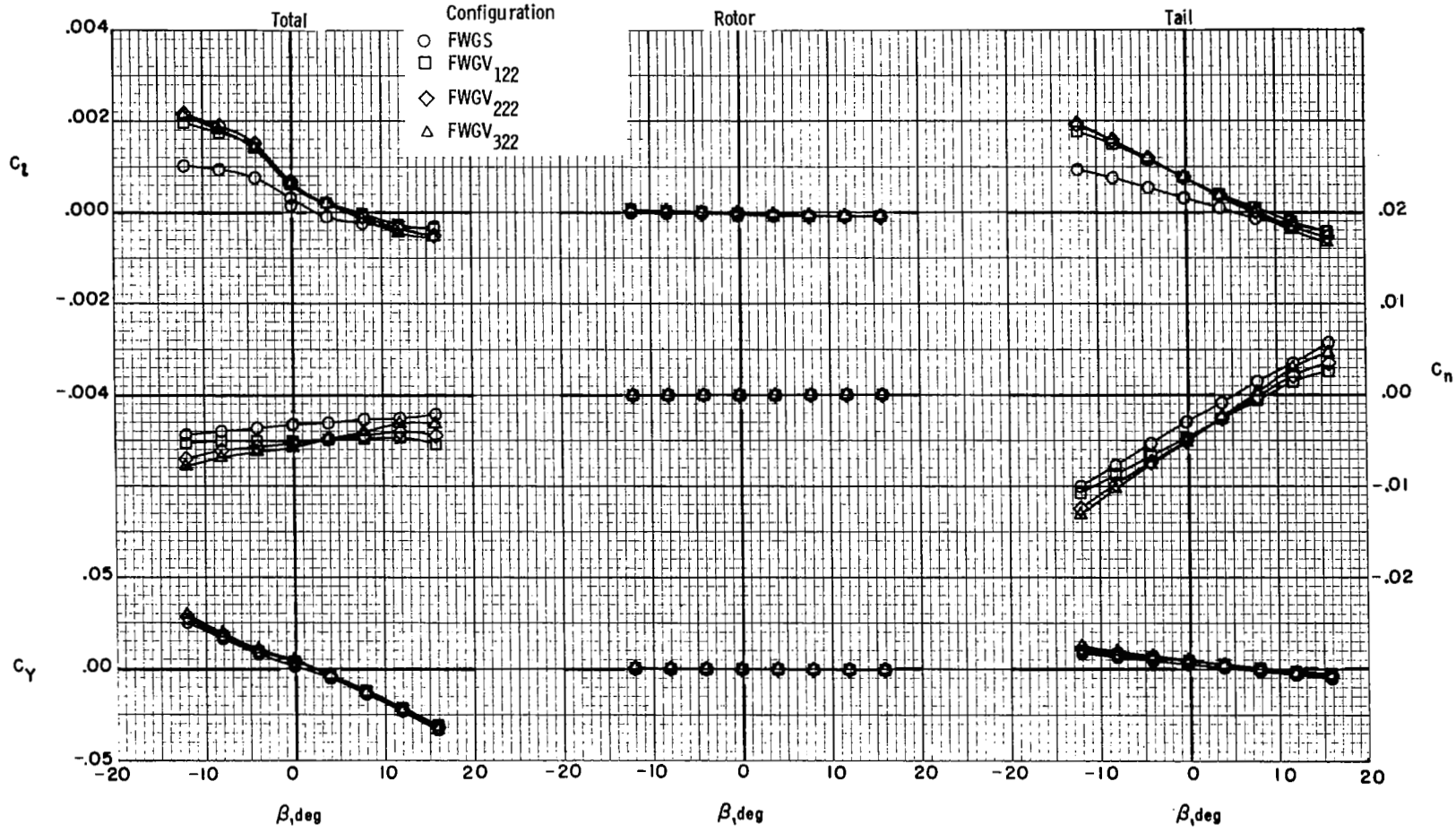

(d) S_2; $i_V = 8^o$.

Figure 11.- Continued.

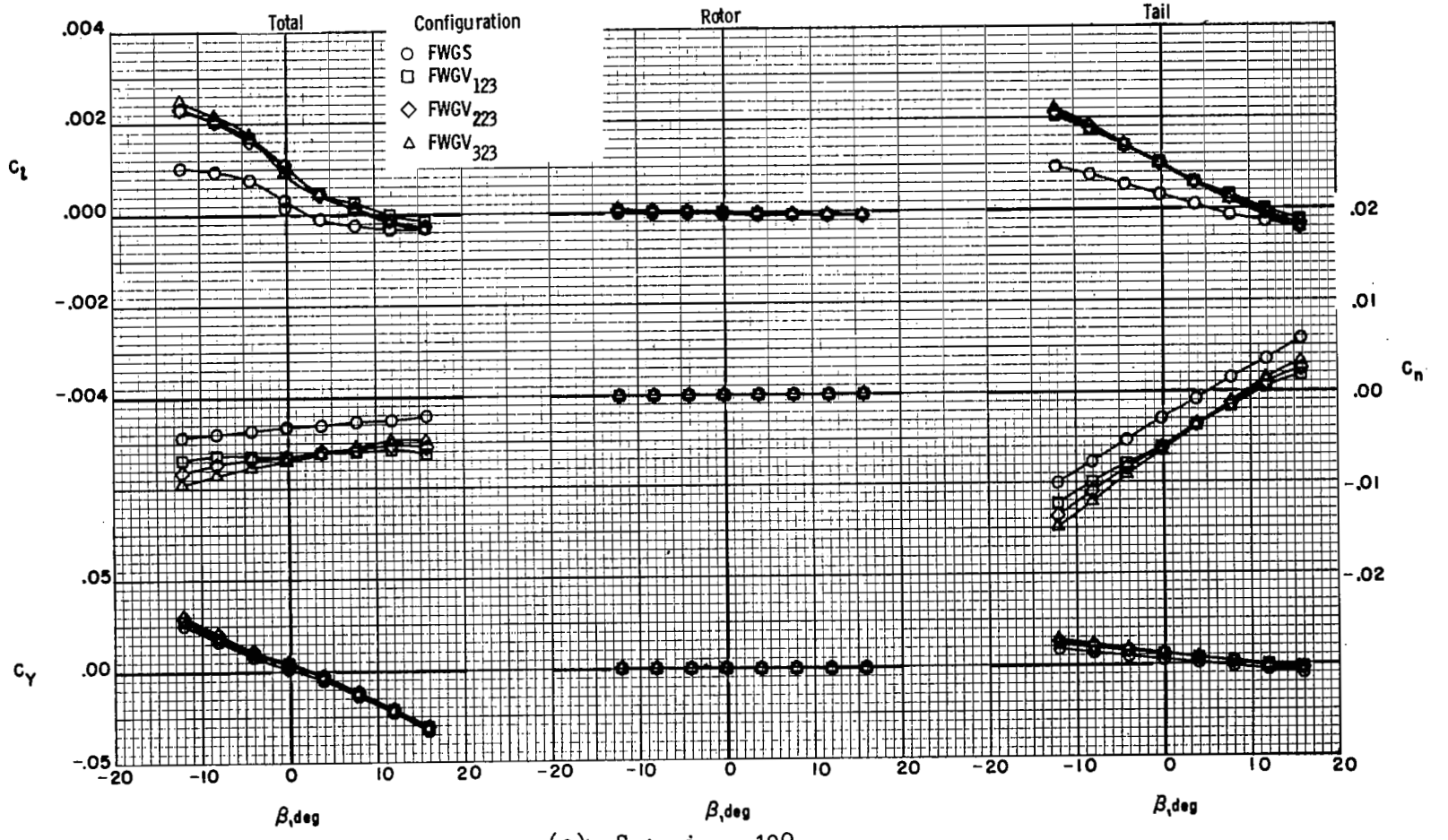

(e) S_2; $i_V = 10^o$.

Figure 11.- Concluded.

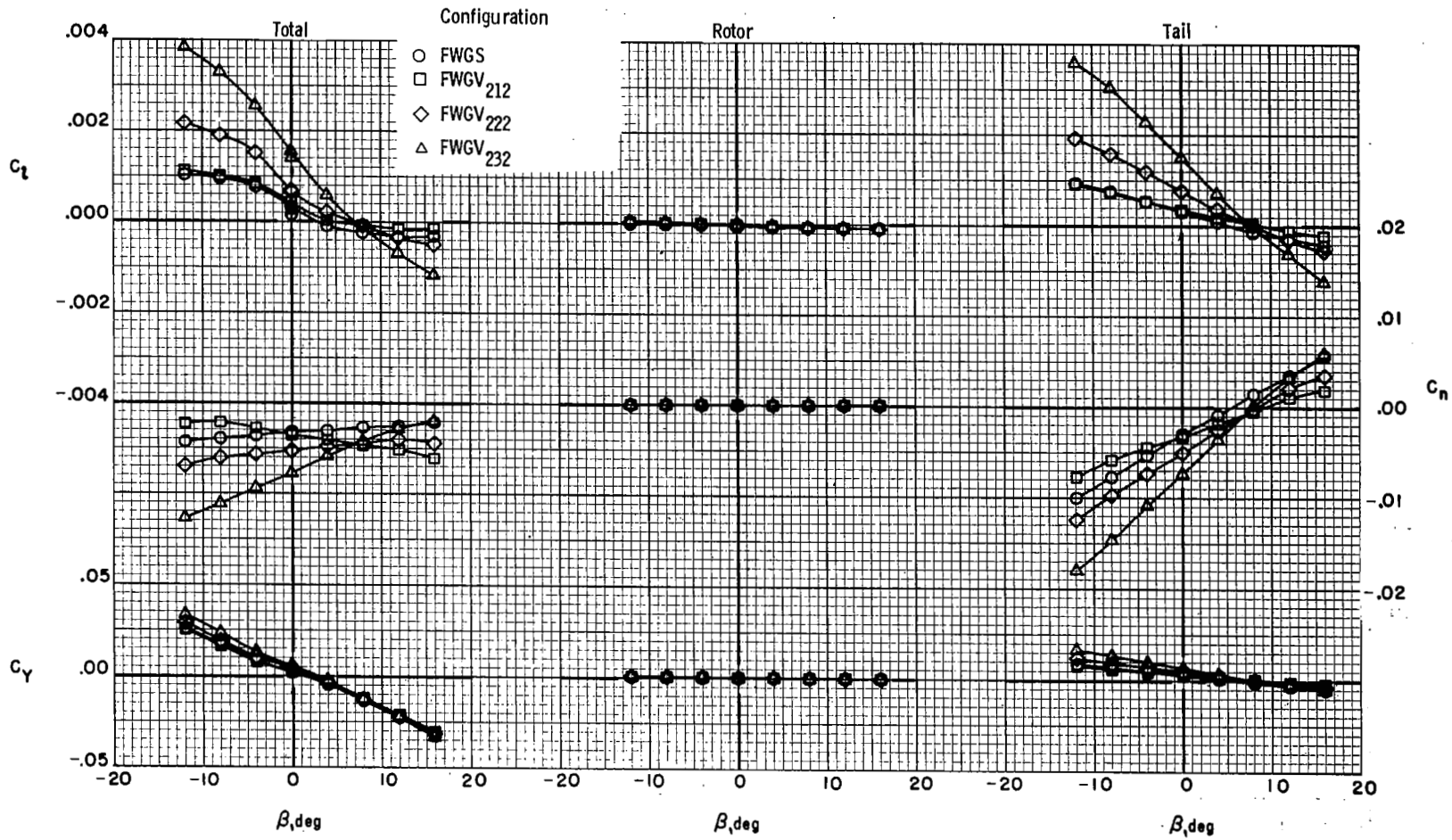

(a) $\Gamma = 50^{o}$; $i_V = 8^{o}$.

Figure 12.- Effect of V-tail planform area on model lateral-directional characteristics.

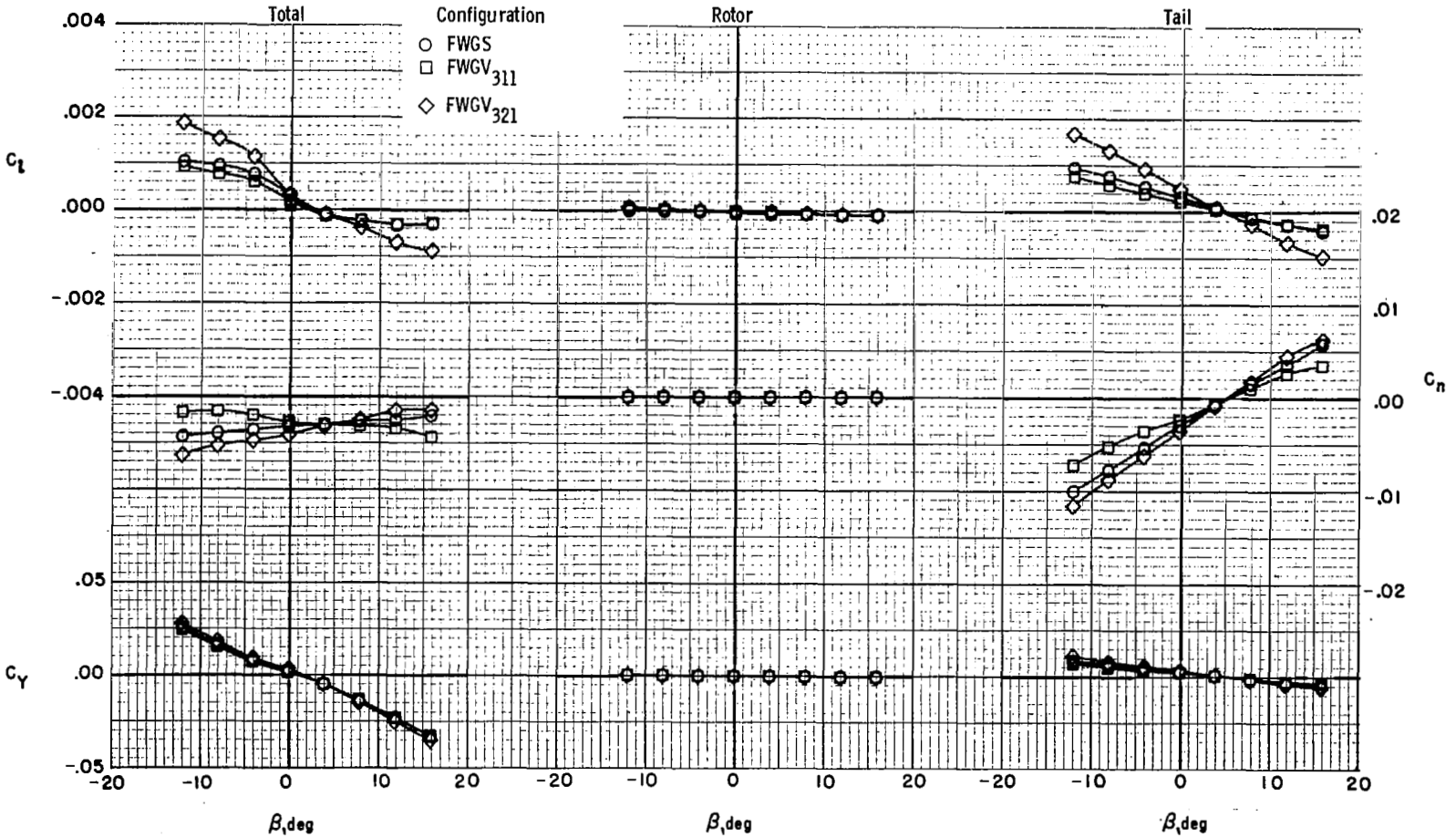

(b) $\Gamma = 55^{\circ}$; $i_V = 5^{\circ}$.

Figure 12.- Continued.

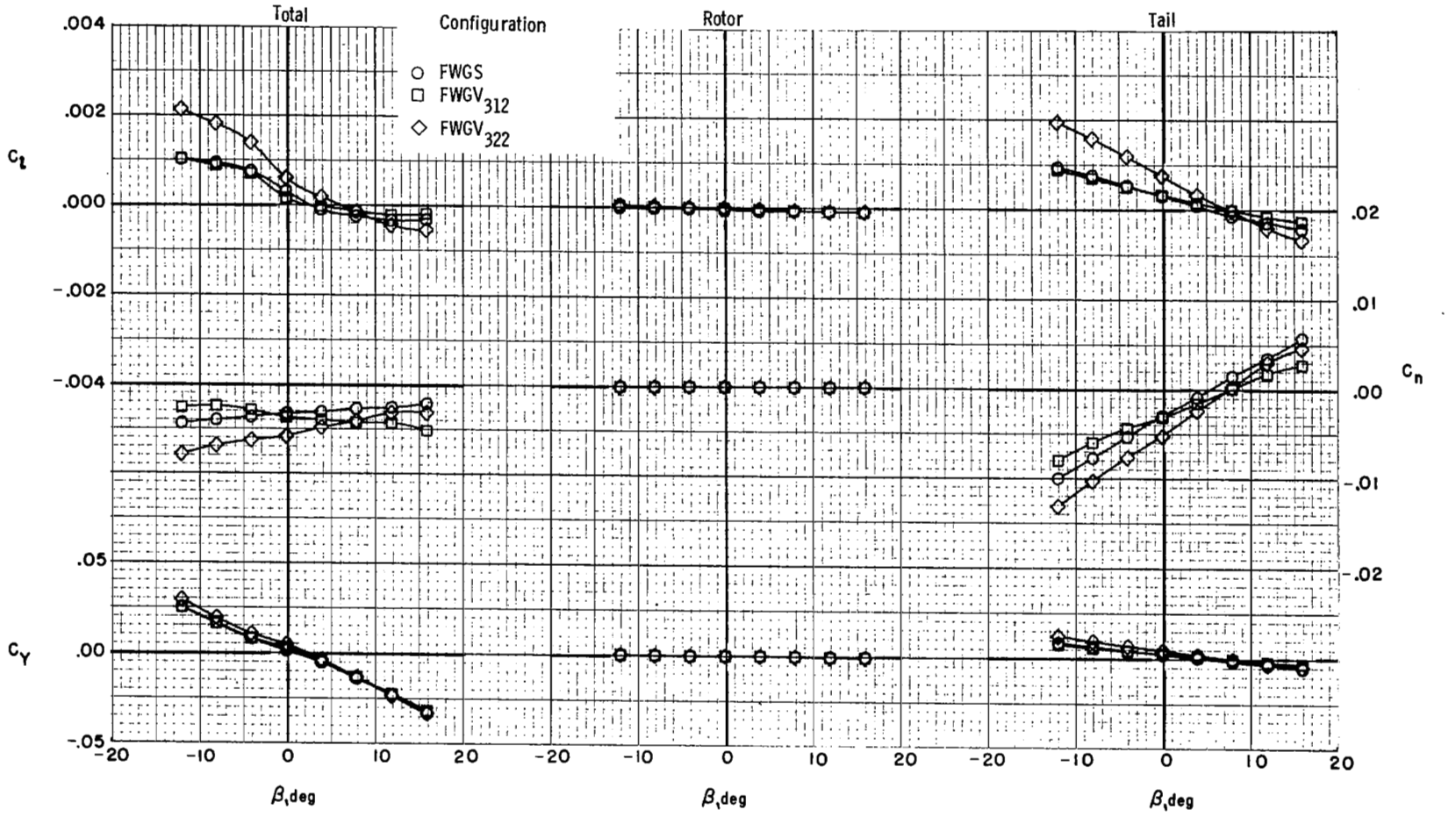

(c) $\Gamma = 55^{\circ}$; $i_V = 8^{\circ}$.

Figure 12.- Continued.

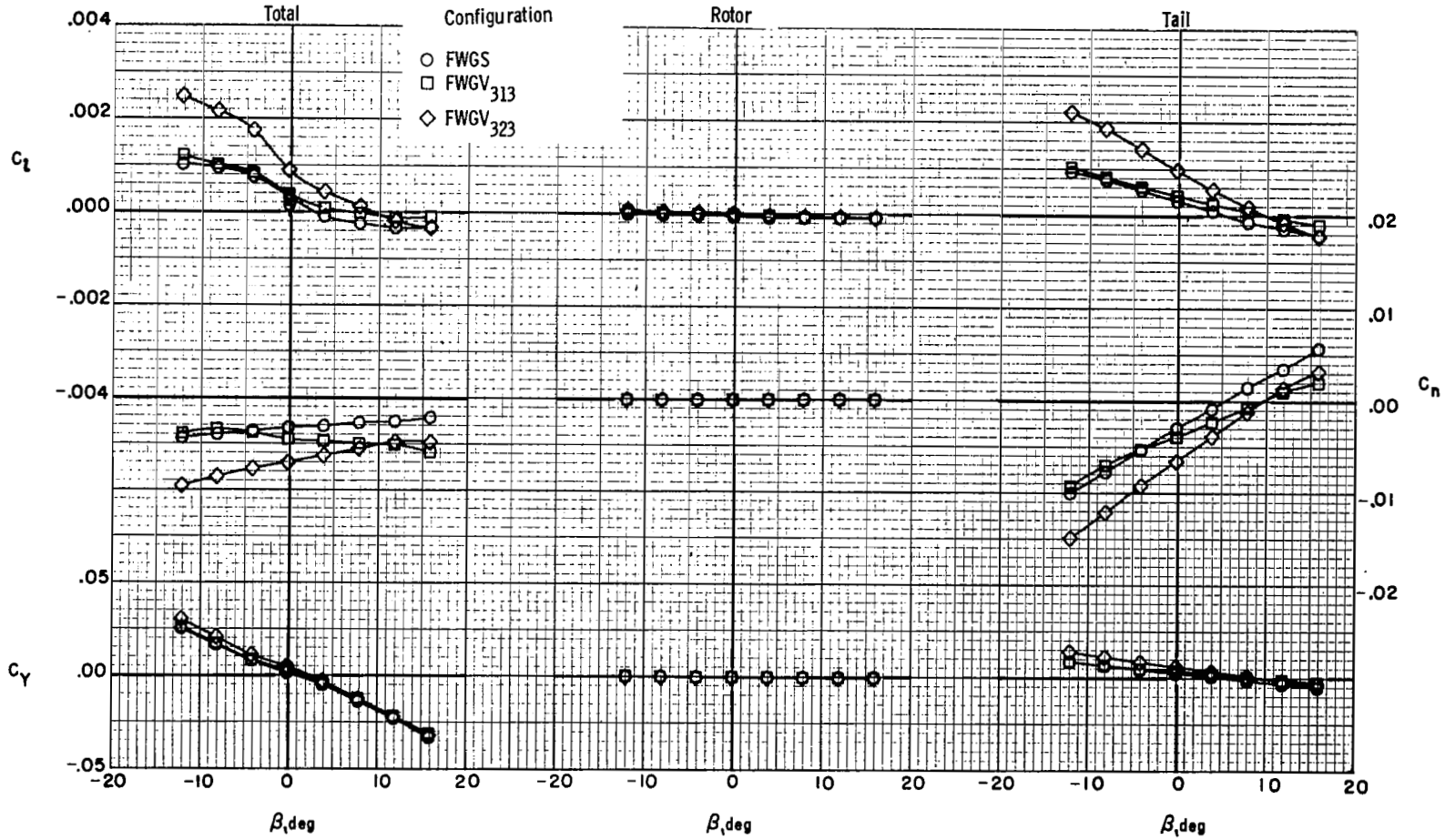

(d) $\Gamma = 55^{\circ}$; $i_V = 10^{\circ}$.

Figure 12.- Concluded.

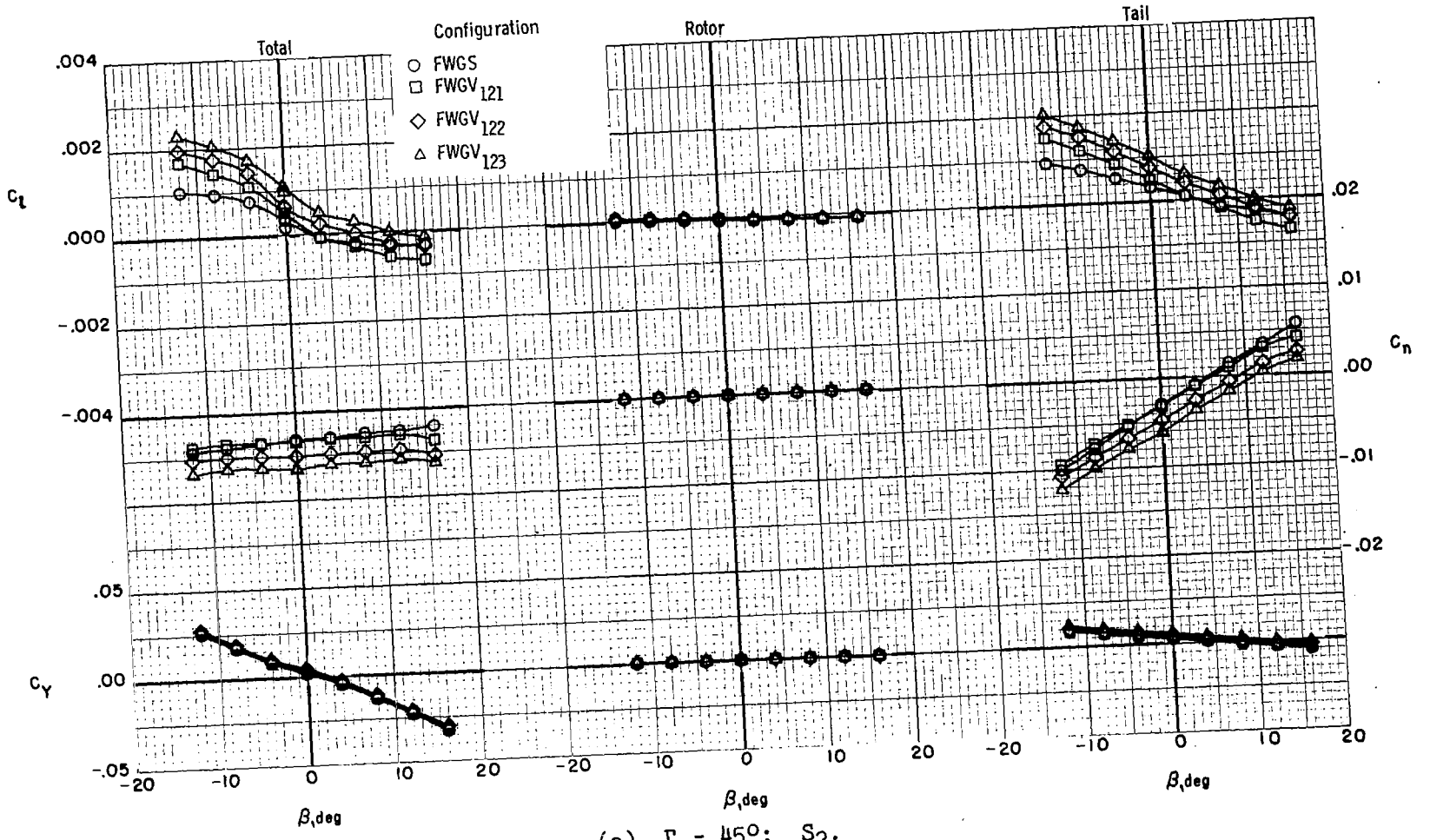

(a) $\Gamma = 45^{o}$; S_2.

Figure 13.- Effect of V-tail incidence angle on model lateral-directional characteristics.

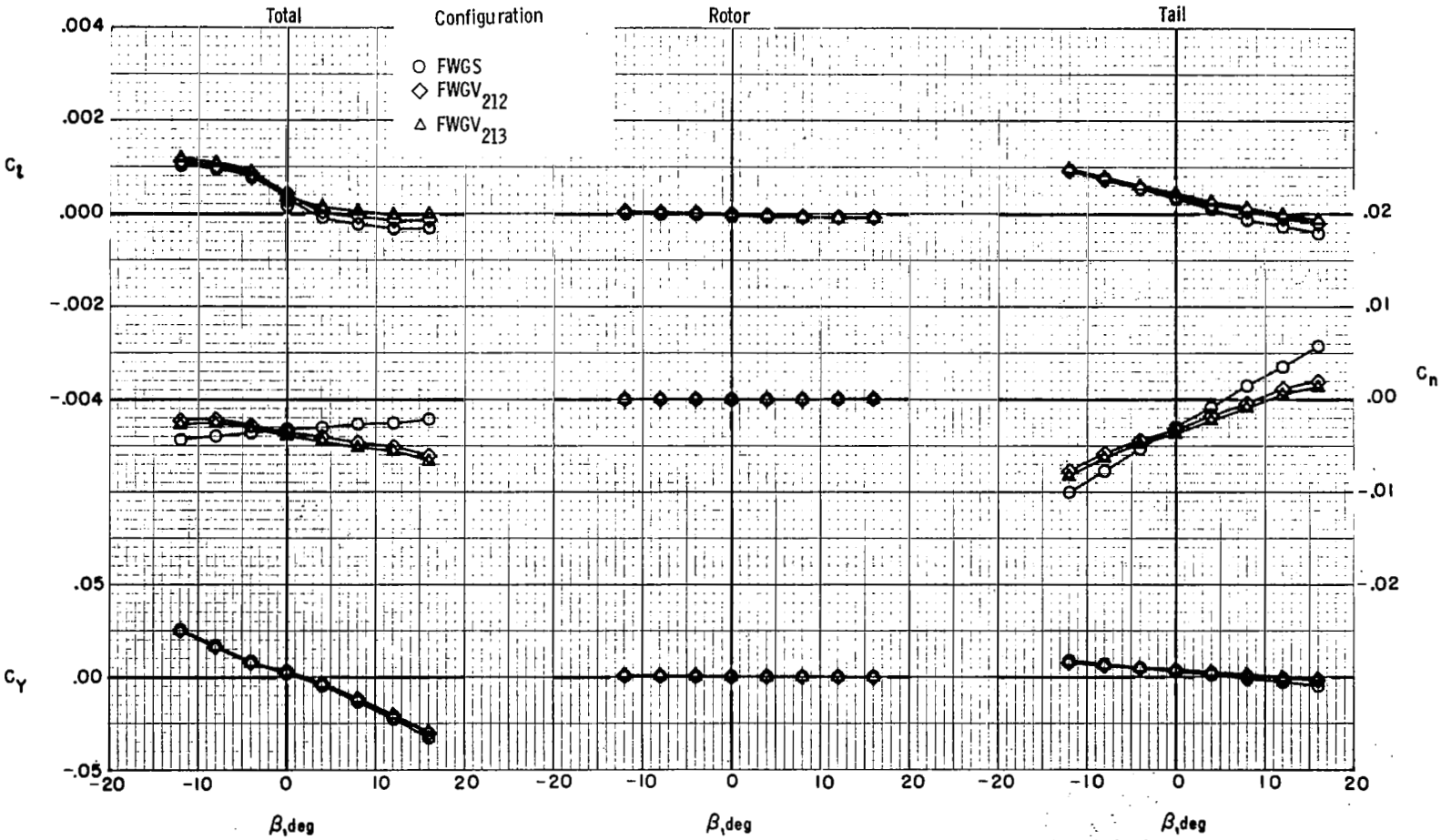

(b) $\Gamma = 50^{\circ}$; S_1.

Figure 13.- Continued.

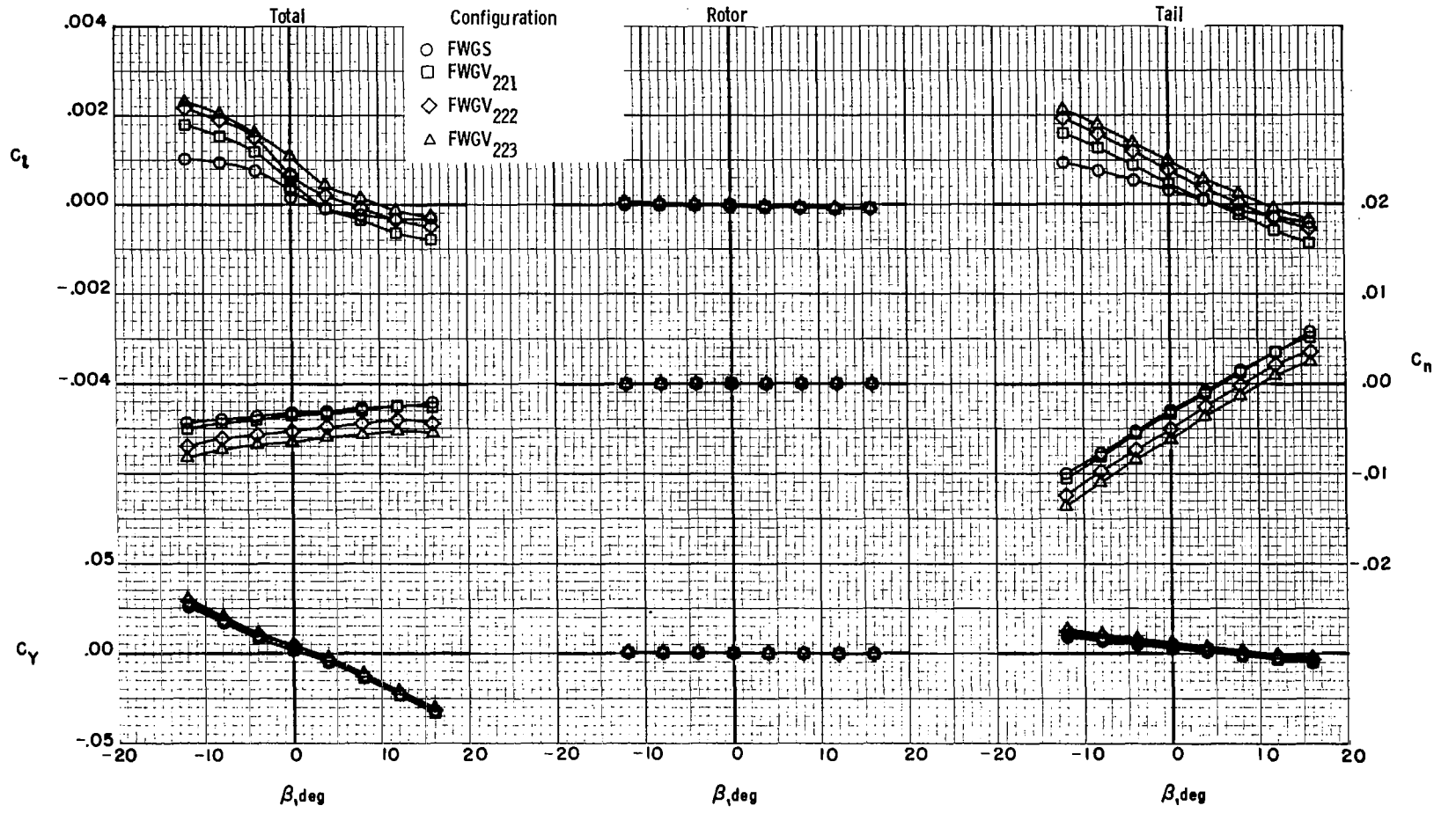

(c) $\Gamma = 50^{o}$; S_2.

Figure 13.- Continued.

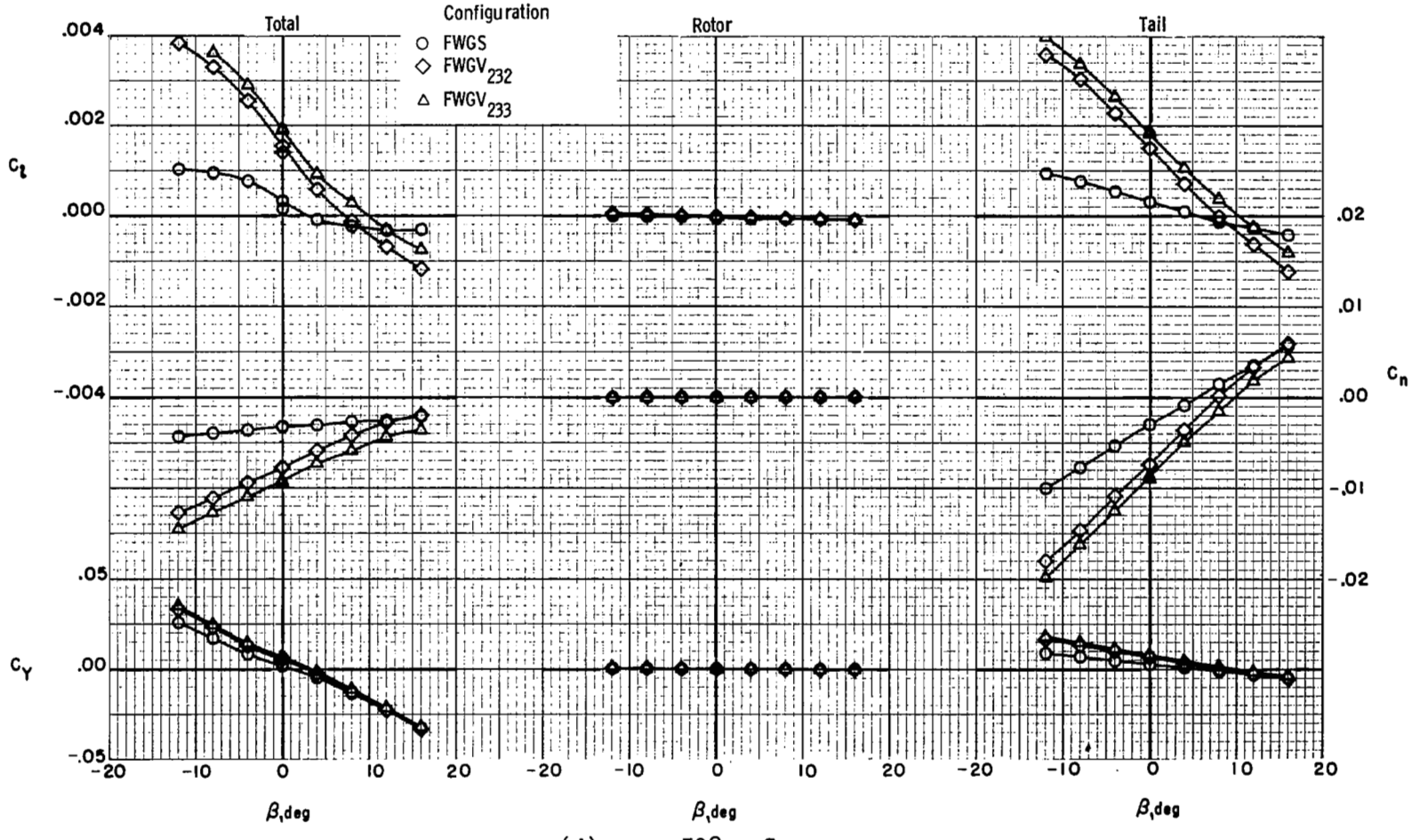

(d) $\Gamma = 50^{\circ}$; S_3.

Figure 13.- Continued.

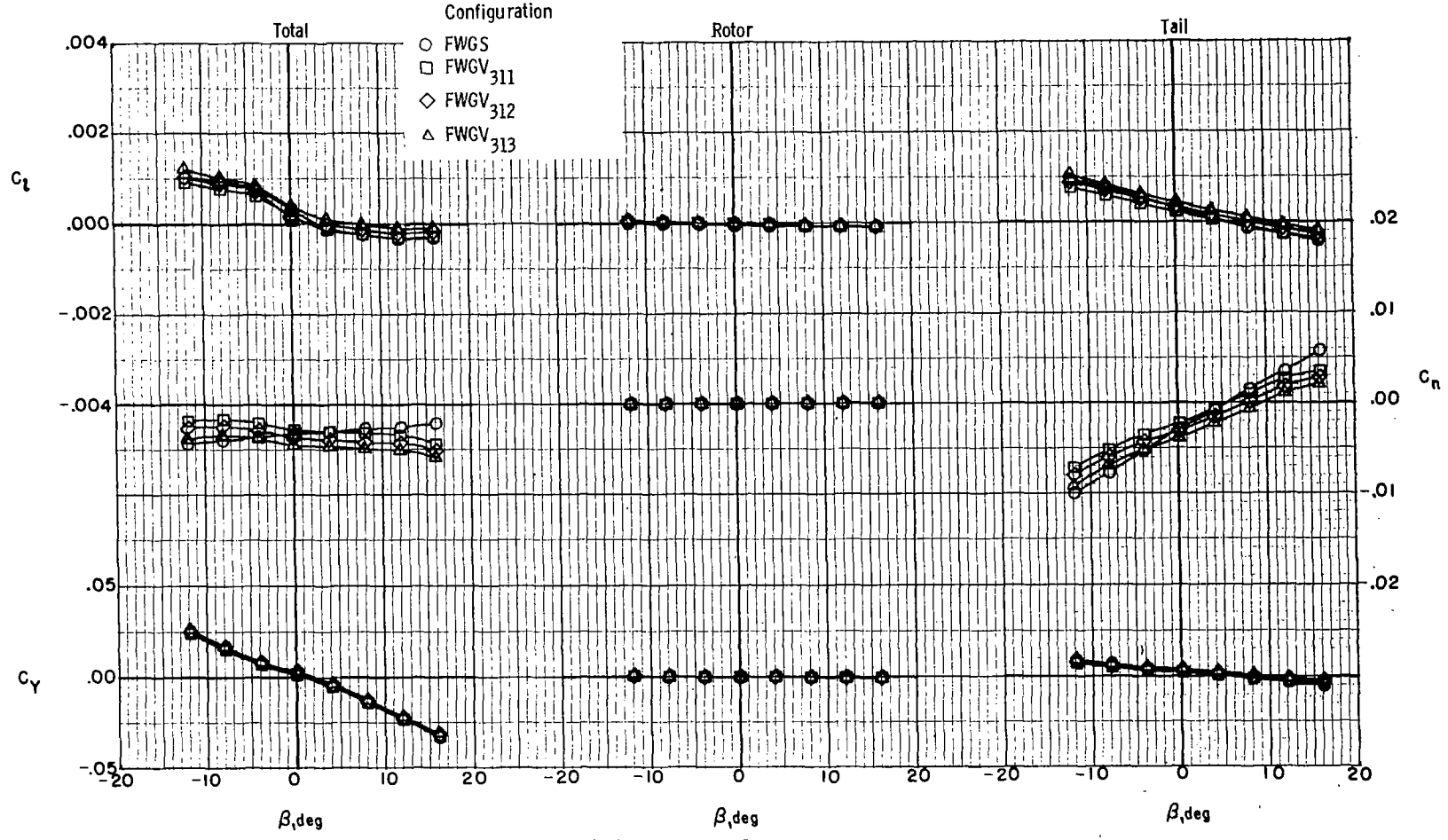

(e) $\Gamma = 55^{\circ}$; S_1.

Figure 13.- Continued.

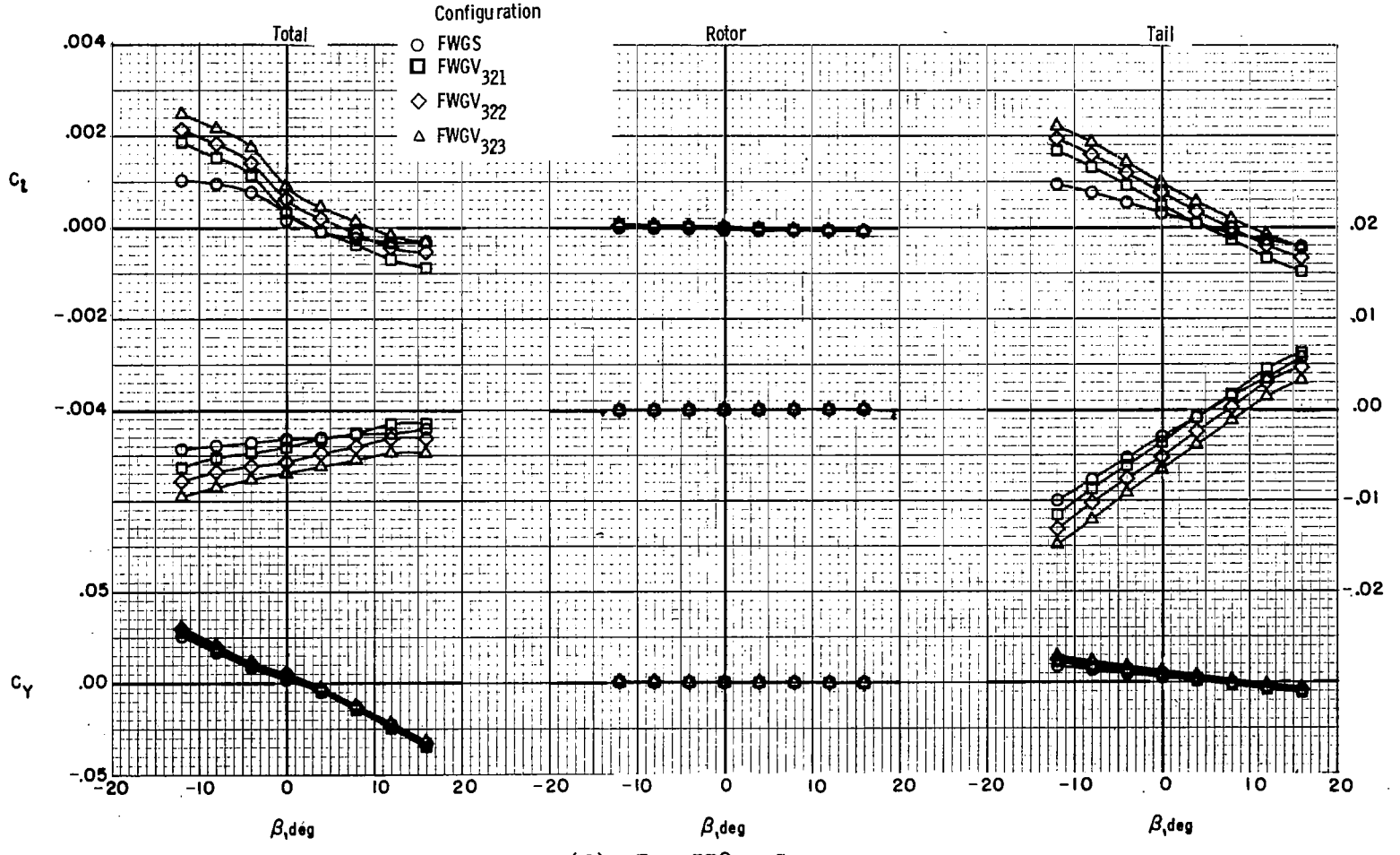

(f) $\Gamma = 55^{\circ}$; S_2.

Figure 13.- Concluded.

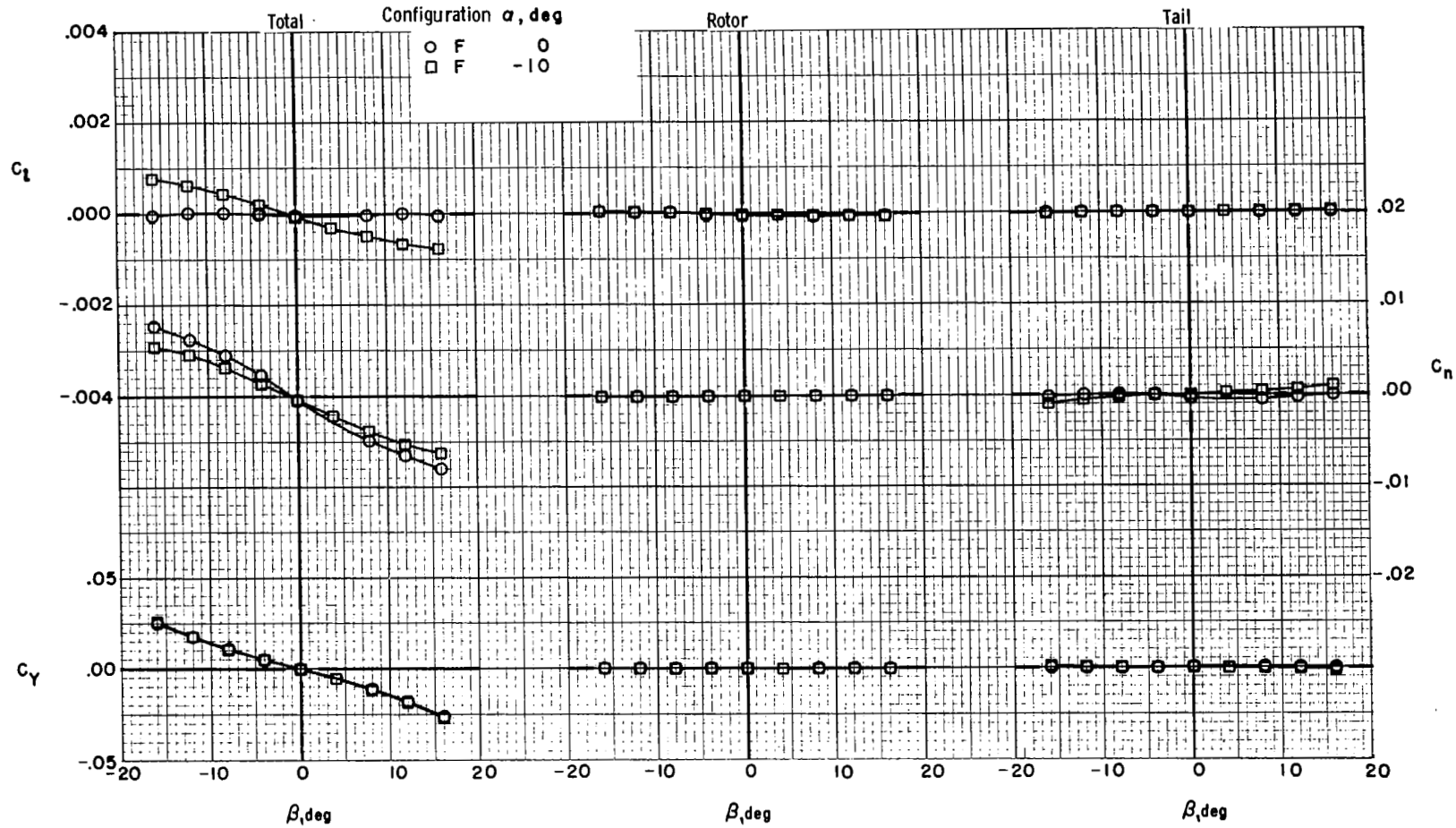

(a) Fuselage alone.

Figure 14.- Effect of angle of attack on model lateral-directional characteristics.

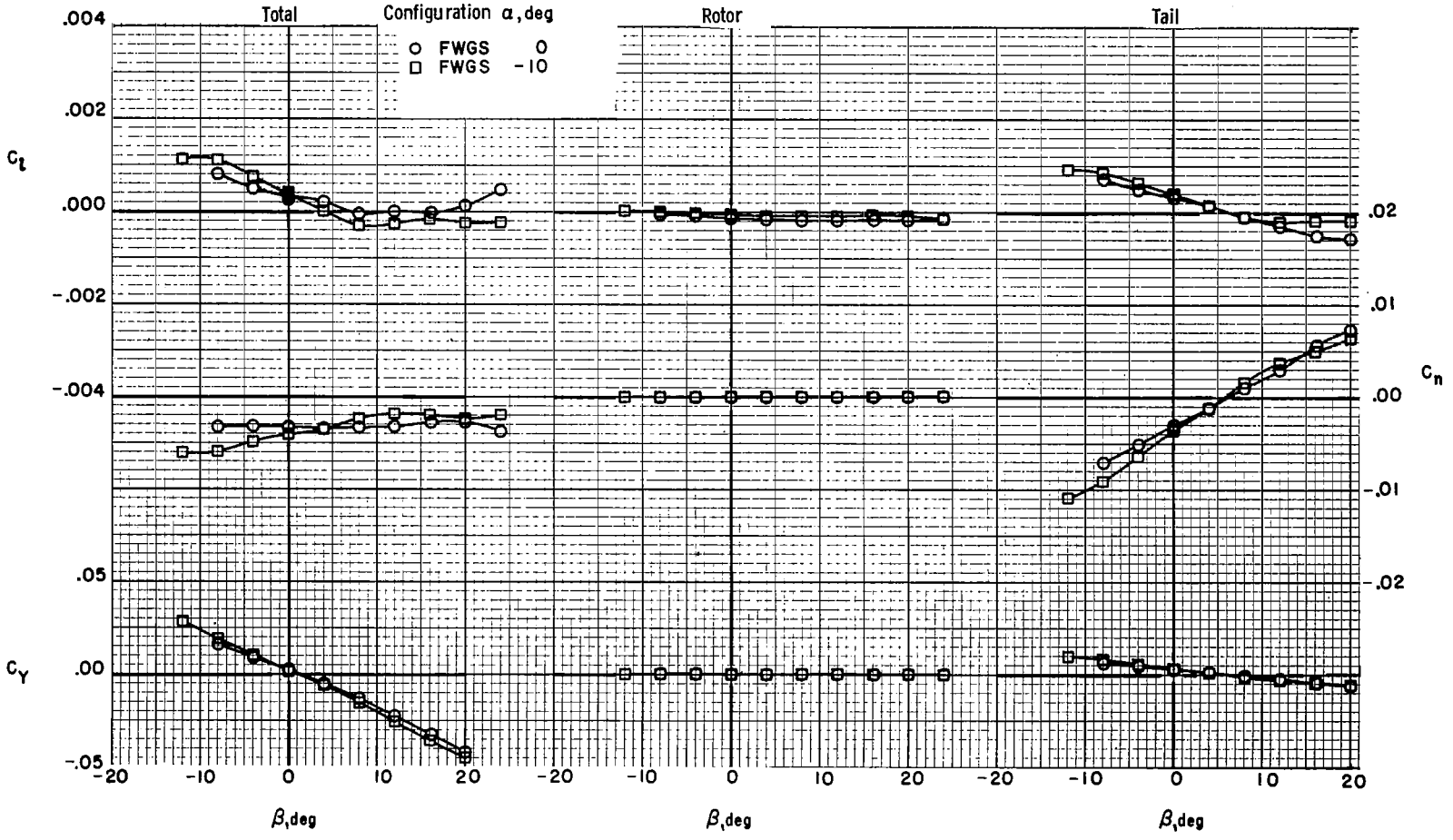

(b) Conventional tail.

Figure 14.- Continued.

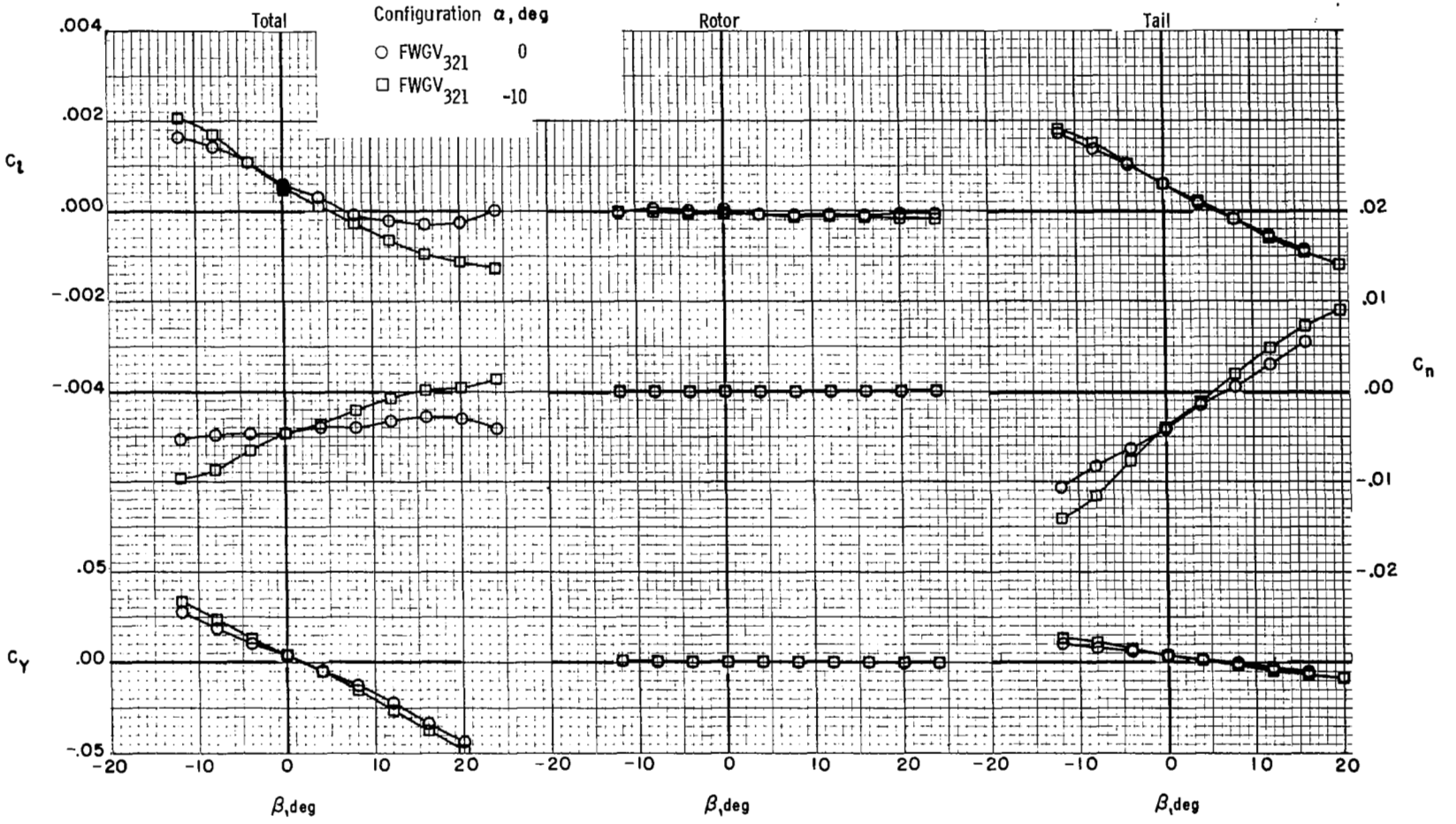

(c) V-tail.

Figure 14.- Concluded.

"The aeronautical and space activities of the United States shall be conducted so as to contribute . . . to the expansion of human knowledge of phenomena in the atmosphere and space. The Administration shall provide for the widest practicable and appropriate dissemination of information concerning its activities and the results thereof."

—NATIONAL AERONAUTICS AND SPACE ACT OF 1958

NASA SCIENTIFIC AND TECHNICAL PUBLICATIONS

TECHNICAL REPORTS: Scientific and technical information considered important, complete, and a lasting contribution to existing knowledge.

TECHNICAL NOTES: Information less broad in scope but nevertheless of importance as a contribution to existing knowledge.

TECHNICAL MEMORANDUMS: Information receiving limited distribution because of preliminary data, security classification, or other reasons. Also includes conference proceedings with either limited or unlimited distribution.

CONTRACTOR REPORTS: Scientific and technical information generated under a NASA contract or grant and considered an important contribution to existing knowledge.

TECHNICAL TRANSLATIONS: Information published in a foreign language considered to merit NASA distribution in English.

SPECIAL PUBLICATIONS: Information derived from or of value to NASA activities. Publications include final reports of major projects, monographs, data compilations, handbooks, sourcebooks, and special bibliographies.

TECHNOLOGY UTILIZATION PUBLICATIONS: Information on technology used by NASA that may be of particular interest in commercial and other non-aerospace applications. Publications include Tech Briefs, Technology Utilization Reports and Technology Surveys.

Details on the availability of these publications may be obtained from:

SCIENTIFIC AND TECHNICAL INFORMATION OFFICE

NATIONAL AERONAUTICS AND SPACE ADMINISTRATION

Washington, D.C. 20546